Robust Isenthalpic Flash for Multiphase Water/Hydrocarbon Mixtures

Di Zhu and **Ryosuke Okuno,** University of Alberta

Summary

Robust isenthalpic flash is important in compositional simulation of steam injection, which involves at least three phases—oleic, gaseous, and aqueous. However, multiphase isenthalpic flash is challenging because the total enthalpy can be substantially nonlinear, or even discontinuous, with respect to temperature. This type of phase behavior is referred to as narrow-boiling behavior in the literature.

This paper presents robust isenthalpic flash for multiphase water-containing hydrocarbon mixtures. The algorithm developed is based on the direct substitution (DS) presented in our previous research for two phases. A detailed analysis is given for narrow-boiling behavior and its effects on the DS algorithm. A new method is also presented for *K*-value estimates for three phases for water-hydrocarbon mixtures. The thermodynamic model used is the Peng-Robinson equation of state with the van der Waals mixing rules.

The narrow-boiling behavior in isenthalpic flash occurs when a small temperature change yields significant changes of equilibrium-phase compositions relative to the overall composition. The system of equations used in the DS algorithm becomes degenerate for narrow-boiling fluids. The multiphase DS algorithm developed in this paper adaptively switches between Newton's iteration step and the bisection step depending on the Jacobian condition number. The bisection algorithm solves for temperature, based solely on the enthalpy constraint only when narrow-boiling behavior is identified. The algorithm is tested with a number of different isenthalpic flash calculations for three and four phases formed by water-containing hydrocarbon mixtures at elevated temperatures. Results show the robustness of the algorithm for narrow-boiling fluids, including the cases with one degree of freedom.

Introduction

Steam injection has been widely implemented for heavy-oil and bitumen recovery (Prats 1982; Butler 1991). Vaporization/condensation of light hydrocarbons is one of the recovery mechanisms in steam injection for heavy oil (Willman et al. 1961; Hagoort et al. 1976; Prats 1982; Shu and Hartman 1988; Brantferger et al. 1991; Bruining and Marchesin 2007). Although bitumen contains light hydrocarbons at lower concentrations than heavy oil, the vaporization/condensation mechanism also may be important in steam/solvent coinjection for bitumen recovery (Jha et al. 2013; Keshavarz et al. 2014a). This mechanism involves the complex interaction between reservoir flow and multiphase behavior. Detailed understanding of compositional reservoir flow is important for synergistic usage of thermal and compositional effects on heavy-oil/bitumen recovery.

It is common practice to use a K-value-based phase-behavior model, along with simple mixing rules for phase densities and viscosities, in thermal compositional simulation (Grabowski et al. 1979; Rubin and Buchanan 1985; CMG 2011; Keshavarz et al. 2014b). Use of a cubic equation of state (EOS) in simulation is more time-consuming, but more general than the K-value-based simulation (Ishimoto et al. 1987; Chien et al. 1989; Brantferger et al. 1991; Varavei and Sepehrnoori 2009; Liu et al. 2009). Phase-behavior modeling by use of an EOS is important when the primary focus of flow simulation is on the investigation of detailed recovery mechanisms (Brantferger et al. 1991; Okuno and Xu 2014). Iranshahr et al. (2010) presented an efficient EOS thermal simulator on the basis of phase-behavior parameterization with tie-line information.

A common selection of independent variables in EOS thermal simulation includes the component mole numbers, pressure, and enthalpy for each gridblock (Brantferger et al. 1991; Liu et al. 2009). The use of enthalpy as an independent variable associated with the energy-conservation equation is more general than the use of temperature because the former can naturally accommodate the cases of one degree of freedom (e.g., two-component, three-phase systems) (Brantferger et al. 1991). In this simulation formulation, phase behavior at each gridblock at each timestep is calculated at a given pressure (P), enthalpy (H), and overall composition (i.e., isenthalpic or PH flash).

Multiphase PH flash for narrow-boiling fluids has been a technical issue to be resolved. The term "narrow boiling" is used in the literature to indicate the enthalpy behavior that is substantially sensitive to temperature (Agarwal et al. 1991). The limiting narrow-boiling behavior occurs for one degree of freedom, in which the enthalpy exhibits a discontinuity in temperature space. In such a case, the interdependency of pressure and temperature excludes one of the PH-flash algorithms proposed in the literature, which has pressure-temperature (PT) flash nested in the outer temperature iteration loop (Agarwal et al. 1991; Brantferger et al. 1991; Michelsen 1993; Néron et al. 2012).

The most widely used algorithm for PH flash is the direct-substitution (DS) algorithm, which was originally developed by Michelsen (1987). In this algorithm, the fugacity equations and enthalpy constraint are solved with K values and temperature as independent variables. For each iteration, one Newton's iteration step is performed with the Rachford-Rice equations (Rachford and Rice 1952) and the enthalpy constraint as functions of independent phase mole fractions and temperature. Then, K values are updated on the basis of the temperature change that was obtained by the Newton's iteration step.

The DS algorithm of Michelsen (1987) was modified later by Agarwal et al. (1991). The difference between the DS algorithms of Michelsen and Agarwal et al. is that the latter performs a quasi-Newton update (QNSS) of K values (Nghiem 1983; Nghiem and Li 1984) before the Newton's iteration step for the Rachford-Rice equations and the enthalpy constraint.

Michelsen (1987) and Agarwal et al. (1991) reported that their DS algorithms do not always converge for narrow-boiling fluids. A potential remedy was proposed for the convergence difficulty when temperature oscillations were identified during the DS iteration (Michelsen 1987). However, Zhu and Okuno (2014) demonstrated in their two-phase case studies that the DS algorithms of Michelsen (1987) and Agarwal et al. (1991) can exhibit nonconvergence with Michelsen's remedy. They concluded that temperature oscillation is a consequence of, not the reason for, narrow-boiling behavior. Zhu and Okuno (2014) showed, for two phases, that the system of equations solved in the DS algorithm becomes nearly degenerate for narrow-boiling fluids. Then, they developed a modified two-phase DS algorithm that can adaptively switch between a bisection and a Newton's step depending on the condition number of the Jacobian matrix. The bisection algorithm solves for temperature solely on the basis of the enthalpy constraint

This paper (SPE 170092) was accepted for presentation at the SPE Heavy Oil Conference—Canada, Calgary, 10–12 June 2014, and revised for publication. Original manuscript received for review 24 September 2014. Revised manuscript received for review 12 December 2014. Paper peer approved 22 January 2015.

when narrow-boiling behavior is detected by a large condition number of the Jacobian matrix. The modified DS algorithm successfully solved the two-phase PH flash calculations for which the prior DS algorithms (Michelsen 1987; Agarwal et al. 1991) showed nonconvergence. Although the DS algorithm of Zhu and Okuno (2014) was successfully applied to two phases of simple hydrocarbon mixtures, its robustness is uncertain for practical reservoir-engineering problems (i.e., three and more phases of water-containing hydrocarbon mixtures).

The PH-flash algorithms mentioned previously assume a certain number of equilibrium phases. For the PH specification, the number of equilibrium phases is unknown not only in composition space, but also in temperature space. Gupta et al. (1990, 1991) proposed a novel method for PT flash that combined stability and flash calculations. Gupta et al. (1990) extended their novel methodology to PH flash, in which the enthalpy, Rachford-Rice, and stability equations were solved simultaneously for temperature, phase amounts, and stability variables. K values were then updated in the outer loop. To our knowledge, application of their PH flash has not been reported in the literature since then. Their algorithm exhibited improved robustness in PH flash for systems with one degree of freedom. This is expected because the nonconvergence that occurs for one degree of freedom is caused by misidentification of the number of equilibrium phases. However, narrow-boiling behavior can occur even for a fixed number of phases. One degree of freedom is recognized as the limiting case of narrow-boiling problems, and can be handled by means of stability analysis, as in Gupta et al. (1990), or the DS algorithm, as presented in the current paper.

The main objective of this paper is to develop a robust algorithm for multiphase PH flash that can handle narrow-boiling behavior, including the cases with one degree of freedom. The current paper also aims to address a few unanswered questions regarding PH flash. For example, it is uncertain in the literature whether the DS algorithm can robustly handle fluids with one degree of freedom. Also, Zhu and Okuno (2014) showed that the scaling of temperature and enthalpy can substantially affect the condition number of the Jacobian matrix in the DS algorithm. However, it was not shown how the robustness of the DS algorithm is affected by the scaling. In the subsequent sections, the new multiphase PH-flash algorithm is first presented. Then, the effect of narrow-boiling behavior on PH flash is illustrated with a few examples. Case studies show the robustness of the developed DS algorithm for three and four phases formed by water-containing hydrocarbon mixtures.

Multiphase Direct Substitution (DS) With Adaptive Newton-Bisection

This section first describes the working equations in the DS algorithm for isenthalpic flash for a general N_C-component N_P-phase system, where N_C and N_P are the numbers of components and phases, respectively. Then, the DS algorithm developed is explained in detail for three phases of water-containing hydrocarbon mixtures. The explanation is based on three phases for specificity, but it was extended to four phases, as is shown in the Case Studies section.

There are many thermodynamic models proposed in the literature for water-containing hydrocarbon mixtures. The robustness of isenthalpic (PH) flash algorithms likely depends on the thermodynamic model used because different thermodynamic models give different variations of the Gibbs free energy in composition-temperature space. In this research, the Peng-Robinson (PR) equation of state (EOS) (Peng and Robinson 1976a, b) is used with the van der Waals mixing rules.

The isenthalpic-flash formulation is presented in Appendix A. The PH-flash calculations in this research consider mutual solubilities of water and hydrocarbons. Particularly, water solubilities in the oleic (L) phase may not be ignored at elevated temperatures, as observed by a number of authors (e.g., Griswold and Kasch 1942; Tsonopoulos and Wilson 1983; Heidman et al. 1985; Glandt and Chapman 1995; Economou et al. 1997; Tsonopoulos 1999; Amani et al. 2013a, b). The binary interaction parameters (BIPs) for water with n-alkanes are taken from the correlation of Venkatramani and Okuno (2014). Their BIP correlation was developed on the basis of BIP values that were optimized in terms of three-phase predictions for water/n-alkane binaries by use of the PR EOS with the van der Waals mixing rules. PH flash in this research solves for three and more equilibrium phases as predicted by the PR EOS, instead of assuming the complete immiscibility between the L and W phases.

The DS algorithm searches for K values and T that satisfy Eqs. A-2 through A-4 (see Appendix A) and the fugacity equations,

$$f_{ij} = \ln(x_{ij}\varphi_{ij}) - \ln(x_{iN_P}\varphi_{iN_P}) = 0 \text{ for } i = 1, 2, \ldots, N_C, \text{ and } j = 1, 2, \ldots, N_P - 1, \quad \ldots\ldots\ldots (1)$$

where φ_{ij} is the fugacity coefficient of component i in phase j and x_{ij} is the mole fraction of component i in phase j. The K value of component i in phase j is defined as

$$K_{ij} = x_{ij}/x_{iN_P}, \quad \ldots\ldots\ldots\ldots\ldots\ldots\ldots\ldots (2)$$

where $i = 1, 2, \ldots, N_C$, and $j = 1, 2, \ldots, (N_P - 1)$. The N_Pth phase is the reference phase in Eqs. 1 and 2.

K values are related to the mole fraction of phase j (β_j) and x_{ij} through the Rachford-Rice equations; that is, β_j can be obtained from solution of the Rachford-Rice equations. The Rachford-Rice equations are

$$g_j = \sum_{i=1}^{N_C}\left(x_{ij} - x_{iN_P}\right) = \sum_{i=1}^{N_C}\left(K_{ij} - 1\right)z_i/t_i = 0 \text{ for } j = 1, 2, \ldots, (N_P - 1), \quad \ldots\ldots\ldots\ldots (3)$$

where $t_i = 1 + \sum_{j=1}^{N_P-1}(K_{ij} - 1)\beta_j$ for $i = 1, 2, \ldots, N_C$ (Okuno 2009; Okuno et al. 2010), and z_i is the overall mole fraction of component i. Then, the corresponding x_{ij} can be obtained from $x_{iN_P} = z_i/t_i$ and Eq. 2 for $j \neq N_P$.

The DS algorithm in this research uses the enthalpy constraint in a dimensionless form:

$$g_{N_P} = \left(\underline{H}^t - \underline{H}_{\text{spec}}\right)/\underline{H}_{\text{spec}} = \underline{H}^t_D - 1.0 = 0, \quad \ldots\ldots\ldots (4)$$

where $\underline{H}^t$ is the total molar enthalpy, $\underline{H}_{\text{spec}}$ is the specified molar enthalpy, and $\underline{H}^t_D = \underline{H}^t/\underline{H}_{\text{spec}}$. The system of N_P dimensionless equations (Eqs. 3 and 4) is solved for dimensionless variables T_D and β_j ($j = 1, 2, \ldots, N_P - 1$) on the basis of Newton's method for root-finding, where $T_D = T/T_{\text{ref}}$. T_{ref} is some reference value to make temperature better scaled in PH flash. For example, T_{ref} can be a temperature near the original reservoir temperature in thermal-oil-recovery processes (e.g., 300 K, as used in this paper). The Jacobian matrix required is presented in Appendix B for a general N_C-component N_P-phase system. The W phase is considered as the reference phase throughout this research.

The multiphase DS algorithm in this paper is an extension of the two-phase DS algorithm presented in Zhu and Okuno (2014). The main advantage over other multiphase DS algorithms lies in how it handles narrow-boiling behavior. The DS algorithm in this paper checks for the narrow-boiling behavior on the fly on the basis of the condition number of the Jacobian matrix. When near-degeneracy of the system of equations is detected by a large condition number (e.g., greater than 10^6), a robust bisection algorithm solves for T_D solely on the basis of the enthalpy constraint (Eq. 4). This decoupling of T_D from the other variables, β's, is performed only if the system of equations is nearly degenerate. Otherwise, the normal Newton's iteration step is used. That is, the algorithm adaptively switches between Newton's iteration step and the bisection method. Also, the upper and lower temperature limits (T^U_D and T^L_D) are used to avoid having unrealistic temperature values during the iterations.

A stepwise description of the three-phase DS algorithm is given next. The algorithm has been extended to four phases, and a four-phase calculation involving narrow-boiling behavior is shown in the Case Studies section.

- Step 1. Specify $\underline{H}_{spec}$, P, and z_i, along with model parameters such as critical temperature T_C, critical pressure P_C, acentric factor ω, and $N_C \times N_C$ BIPs.
- Step 2. Enter an initial guess for dimensionless temperature, $T_D^{(1)}$, where the number in the bracket represents the iteration-step number $k=1$. Calculate initial estimates for K values [$K_{iL}^{(k)}$ and $K_{iV}^{(k)}$].
- Step 3. Solve Eq. 3 with N_P of three [$g_1^{(k)}$ and $g_2^{(k)}$] for the liquid and vapor phase mole fractions [$\beta_L^{(k)}$ and $\beta_V^{(k)}$] for the kth iteration step so that $|g_1^{(k)}| < \varepsilon_m$ and $|g_2^{(k)}| < \varepsilon_m$ (e.g., $\varepsilon_m = 10^{-10}$). Calculate the corresponding $x_{ij}^{(k)}$.
- Step 4. Calculate the residual of the enthalpy constraint [Eq. 4 with N_P of three, i.e., $g_3^{(k)}$]. If $|g_3^{(k)}|$ is less than the tolerance ε_h, stop (e.g., $\varepsilon_h = 10^{-10}$). Otherwise, continue to Step 5.
- Step 5. Calculate $\ln\varphi_{ij}{}^{(1)}$ and phase heat capacities [$C_{Pj}^{(1)}$] for $j = L$, V, and W.
- Step 6. Calculate the residuals of the fugacity equations [Eq. 1 with N_P of three; i.e., $f_{iL}^{(k)}$ and $f_{iV}^{(k)}$].
- Step 7. Calculate $T_D^{(2)} = T_D^{(1)} - [\underline{H}_{spec} g_3^{(1)}]/(T_{ref}\sum_j \beta_j C_{Pj})^{(1)}$, and initial estimates for K values [Eq. 2 with N_P of three; i.e., $K_{iL}^{(2)}$ and $K_{iV}^{(2)}$].
- Step 8. Solve Eq. 3 with N_P of three [$g_1^{(k)}$ and $g_2^{(k)}$] for $\beta_L^{(k)}$ and $\beta_V^{(k)}$ for the kth iteration step so that $|g_1^{(k)}| < \varepsilon_m$ and $|g_2^{(k)}| < \varepsilon_m$. Calculate the corresponding $x_{ij}^{(k)}$.
- Step 9. Calculate $g_3^{(k)}$, $f_{iL}^{(k)}$, and $f_{iV}^{(k)}$. If $|g_3^{(k)}| < \varepsilon_h$, $|f_{iL}^{(k)}| < \varepsilon_f$, and $|f_{iV}^{(k)}| < \varepsilon_f$ (e.g., $\varepsilon_f = 10^{-10}$) for $i = 1, 2, \ldots, N_C$, stop. Otherwise, continue to Step 10.
- Step 10. Perform a QNSS step for intermediate K values, $K_{ij}^{(k+0.5)}$ for $j = L$ and V;

$$\ln\vec{K}_j^{(k+0.5)} = \ln\vec{K}_j^{(k)} + \frac{[\ln\vec{K}_j^{(k)} - \ln\vec{K}_j^{(k-1)}]^T \vec{f}_j^{(k-1)}}{[\ln\vec{K}_j^{(k)} - \ln\vec{K}_j^{(k-1)}]^T [\vec{f}_j^{(k)} - \vec{f}_j^{(k-1)}]} \vec{f}_j^{(k)}, \quad \ldots\ldots\ldots\ldots\ldots\ldots (5)$$

  where $\vec{K}_j$ and $\vec{f}_j$ are vectors consisting of N_C K values and N_C fugacity equations for phase j, respectively.
- Step 11. Calculate $x_{ij}^{(k+0.5)}$ on the basis of $\beta_L^{(k)}$, $\beta_V^{(k)}$, $K_{iL}^{(k+0.5)}$, and $K_{iV}^{(k+0.5)}$.
- Step 12. Construct the 3×3 Jacobian matrix on the basis of $x_{ij}^{(k+0.5)}$.
- Step 13. Perform one Newton's iteration step to obtain $\beta_L^{(k+1)}$, $\beta_V^{(k+1)}$, and $T_D^{(k+1)}$.
- Step 14. Check to see if $T_D^L < T_D^{(k+1)} < T_D^U$. If so, continue to Step 15. Otherwise, calculate $T_D^{(k+1)}$ with the Regula Falsi method. Then, solve Eqs. 3 with N_P of three [$g_1^{(k)}$ and $g_2^{(k)}$] for $\beta_L^{(k+1)}$ and $\beta_V^{(k+1)}$ for the $(k+1)$th iteration step so that $|g_1^{(k+1)}| < \varepsilon_m$ and $|g_2^{(k+1)}| < \varepsilon_m$. Calculate the corresponding $x_{ij}^{(k+1)}$.
- Step 15. Calculate $g_3^{(k+1)}$, $f_{iL}^{(k+1)}$, and $f_{iV}^{(k+1)}$. If $|g_3^{(k+1)}| < \varepsilon_h$, $|f_{iL}^{(k+1)}| < \varepsilon_f$, and $|f_{iV}^{(k+1)}| < \varepsilon_f$ for $i = 1, 2, \ldots, N_C$, stop. Otherwise, continue to Step 16.
- Step 16. Calculate the condition number of the Jacobian matrix. If it is greater than 10^6, go to Step 18. Otherwise, continue to Step 17.
- Step 17. Update K values; $\ln K_{ij}^{(k+1)} = \ln K_{ij}^{(k)} + (\partial \ln K_{ij}/\partial T_D)^{(k)}[T_D^{(k+1)} - T_D^{(k)}]$. Go to Step 8 after increasing the iteration step number by one: $k = k+1$.
- Step 18-1. Set t_L to the highest temperature among T_D^L, $T_D^{(k)}$, and $T_D^{(k+1)}$ that gives a negative g_3. Set t_U to the lowest temperature among $T_D^{(k)}$, $T_D^{(k+1)}$, and T_D^U that gives a positive g_3.
- Step 18-2. $T_D^{(k+2)} = 0.5(t_L + t_U)$.
- Step 18-3. Perform PT flash at $T_D^{(k+2)}$ to calculate $\beta_L^{(k+2)}$, $\beta_V^{(k+2)}$ and $x_{ij}^{(k+2)}$ such that $|f_{ij}^{(k+2)}| < \varepsilon_f$ for $i = 1, 2, \ldots, N_C$ and $|g_1^{(k+2)}| < \varepsilon_m$ and $|g_2^{(k+2)}| < \varepsilon_m$.
- Step 18-4. Calculate the condition number of the Jacobian matrix. If it is greater than 10^6, continue to Step 18-5. Otherwise, go to Step 9.
- Step 18-5. Calculate $|g_3^{(k+2)}|$. If $|g_3^{(k+2)}|$ is less than the tolerance ε_h, stop. Otherwise, $t_L = T_D^{(k+2)}$ for $g_3^{(k+2)} < 0$, and $t_U = T_D^{(k+2)}$ for $g_3^{(k+2)} > 0$. Then, go to Step 18-2 after increasing the iteration step number by one: $k = k+1$.

Steps 16 and 18-4 require the condition number of the Jacobian matrix. The condition numbers in these steps are calculated as $||J||_1 \cdot ||J^{-1}||_1$, where $||J||_1$ is the one-norm of the Jacobian matrix J. Later in this paper, condition numbers by use of the one-norm will be compared with more-rigorous condition numbers by use of the singular value decomposition (SVD).

Steps 2, 7, 14, and 18-3 require K-value estimates at a given temperature. In this research, a simple but general method is developed for such K-value estimates for the L, V, and W phases on the basis of the following three assumptions: (i) Raoult's law for the W-V equilibrium relation for water, and for the L-V equilibrium relation for hydrocarbons; (ii) the water concentration in the W phase (x_{wW}) is nearly 100%; and (iii) $K_{iL} = x_{iL}/x_{iW}$ is large for hydrocarbons. That is,

$$K_{wL} \approx x_{wL} \quad \ldots\ldots\ldots\ldots\ldots\ldots\ldots\ldots\ldots (6)$$

$$K_{wV} = x_{wV}/x_{wW} \approx P_w^{vap}/P \quad \ldots\ldots\ldots\ldots\ldots\ldots (7)$$

$$K_{iL} = x_{iL}/x_{iW} \text{ for hydrocarbon component } i \quad \ldots\ldots\ldots (8)$$

$$K_{iV} = x_{iV}/x_{iW} \approx (P_i^{vap}/P)K_{iL} \text{ for hydrocarbon component } i. \quad \ldots\ldots\ldots\ldots (9)$$

The correlation of Eubank et al. (1994) can provide x_{wL} for Eq. 6 as

$$\ln(x_{wL}) = -21.2632 + 5.9473 \times 10^{-2}T - 4.0785 \times 10^{-5}T^2 \quad \ldots\ldots\ldots\ldots\ldots\ldots\ldots\ldots (10)$$

for $T < 550$ K. For simplicity, K_{iL} is assumed to be 10^8 for all hydrocarbon components in this paper, although further improvement is possible by considering the effects of temperature and carbon number on K_{iL}. The vapor pressures of well-defined components can be estimated by use of Wagner's correlation (Wagner 1973; McGarry 1983). Vapor pressures of pseudocomponents are directly calculated from the PR EOS. This method can be also used for the V, L, and W phases in multiphase flash for four and more phases. In a four-phase system consisting of the oleic (L_1), solvent-rich liquid (L_2), V, and W phases, for example, a complete set of K-value estimates is given by the previous method and a certain K-value set for L_1 and L_2.

In Step 14, if $T_D^{(k+1)}$ does not lie between T_D^L and T_D^U, a Regula Falsi iteration step is used to update $T_D^{(k+1)}$ as follows:

$$T_D^{(k+1)} = T_D^L - g_3^{(k)}\left(T_D^L - T_D^U\right)/\left(g_3^L - g_3^U\right), \quad \ldots\ldots\ldots (11)$$

where g_3^L and g_3^U are the dimensionless enthalpy constraints (Eq. 4 with N_P of three) calculated at T_D^L and T_D^U, respectively.

Near-Degeneracy in Narrow-Boiling Regions

As explained earlier, a fluid with narrow-boiling behavior exhibits a significant sensitivity of enthalpy to temperature. Robust PH flash should be able to handle convergence difficulties associated with narrow-boiling behavior. This section presents how narrow-

Component	Mole Fraction	MW (g/mol)	T_C (K)	P_C (bar)	ω	C^0_{P1} J/(mol·K)	C^0_{P2} J/(mol·K^2)	C^0_{P3} J/(mol·K^3)	C^0_{P4} J/(mol·K^4)
Water	0.75	18.015	647.3	220.89	0.344	32.200	1.907×10^{-3}	1.055×10^{-5}	-3.596×10^{-9}
C_3	0.15	44.097	369.8	42.46	0.152	–4.220	3.063×10^{-1}	-1.586×10^{-4}	3.215×10^{-8}
C_{16}	0.10	226.400	717.0	14.19	0.742	–13.000	1.529	-8.537×10^{-4}	1.850×10^{-7}
Binary interaction parameters:									
	Water	C_3	C_{16}						
Water	0.0000	0.6841	0.3583						
C_3	0.6841	0.0000	0.0000						
C_{16}	0.3583	0.0000	0.0000						

MW = molecular weight.

Table 1—Properties for the ternary mixture consisting of water, C_3, and C_{16} (Case 1).

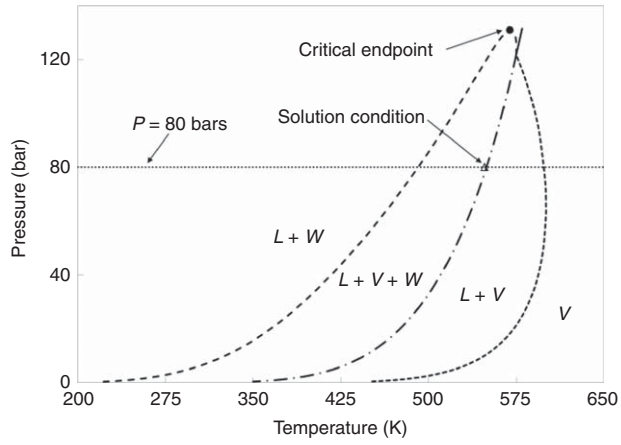

Fig. 1—Phase boundaries in P-T space for a mixture of 75% water, 15% C_3, and 10% C_{16} (Case 1). The properties used for the components are given in Table 1. The critical endpoint of type $L = V + W$ is calculated at 569.35 K and 131.07 bar with the PR EOS.

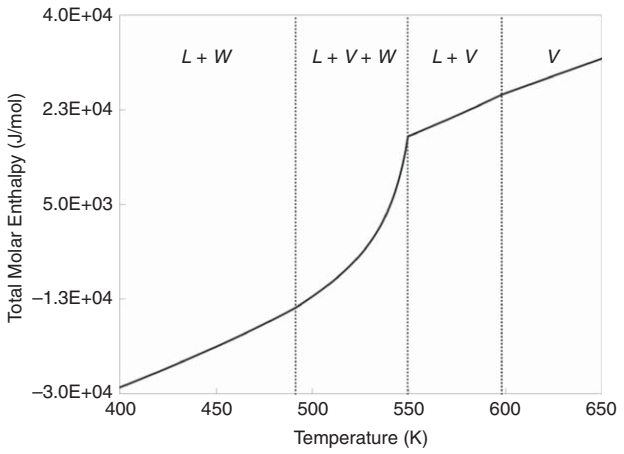

Fig. 2—Total molar enthalpy at 80 bar for a mixture of 75% water, 15% C_3, and 10% C_{16} (Case 1). The properties used for the components are given in Table 1. Three phases are present from 491.17 to 549.25 K. The total molar enthalpy at 80 bar is sensitive to temperature near the phase boundary between $L + V + W$ and $L + V$.

boiling behavior affects the equations solved in the direct-substitution (DS) algorithm for three phases.

Narrow-Boiling Behavior With Three Phases. A characteristic of narrow-boiling behavior is that the amounts of phases (i.e., β's) change rapidly with a small change in temperature, as indicated by its phenomenological name. The amounts of phases depend on the relative location of the overall composition to the equilibrium phases in composition space. This is illustrated next with a simple ternary example (Case 1).

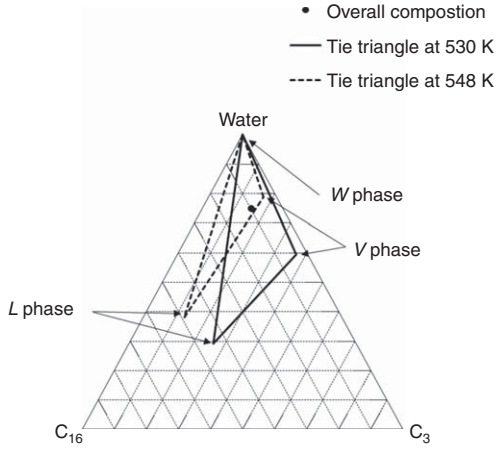

Fig. 3—Tie triangles in composition space at 80 bar at two different temperatures $T_1 = 530$ K and $T_2 = 548$ K. The overall composition is 75% water, 15% C_3, and 10% C_{16} (Case 1). The properties used for the components are given in Table 1.

Case 1 uses a ternary mixture of 75% water (w), 15% propane (C_3), and 10% n-C_{16} (C_{16}), for which properties are given in **Table 1. Fig. 1** shows phase boundaries in P-T space, in which the critical endpoint of type $L = V + W$ is calculated at 569.35 K and 131.07 bar. At 80 bar, three phases exist from 491.17 to 549.25 K. Three-phase PH flash for this mixture is challenging near the boundary between $L + V + W$ and $L + V$ because it presents narrow-boiling behavior. **Fig. 2** shows that $\underline{H}^t$ at 80 bar is sensitive to temperature near the phase boundary.

Fig. 3 presents the tie triangles in composition space at 80 bar at two different temperatures, $T_1 = 530$ K and $T_2 = 548$ K. The three equilibrium phases at T_1 and T_2 are shown as solid and dashed tie triangles, respectively. As temperature increases from T_1 to T_2 ($T_2 - T_1 = 18$ K), the compositions of the L and V phases dramatically change, whereas the W phase stays in the vicinity of the water vertex of composition space. Consequently, the overall composition becomes close to the L-V edge of the tie triangle at T_2. This can be confirmed in Fig. 1, in which T_2 is close to the phase boundary between $L + V + W$ and $L + V$ at 80 bar.

At T_1, the C_3 concentration is 37.03% for the V phase and 26.22% for the L phase, and the C_{16} concentration is 3.51% for the V phase and 44.67% for the L phase. The phase mole fractions are 0.203, 0.261, and 0.536 for the L, V, and W phases, respectively. At T_2, the C_3 concentration is 17.17% for the V phase and 12.76% for the L phase, and the C_{16} concentration is 4.16% for the V phase and 49.21% for the L phase. The phase mole fractions are 0.138, 0.771, and 0.091 for the L, V, and W phases, respectively.

The concentrations of C_3 in the V and L phases decrease rapidly during the temperature increase from T_1 to T_2 ($T_2 - T_1 = 18$ K). This results from the variation of the Gibbs free energy in

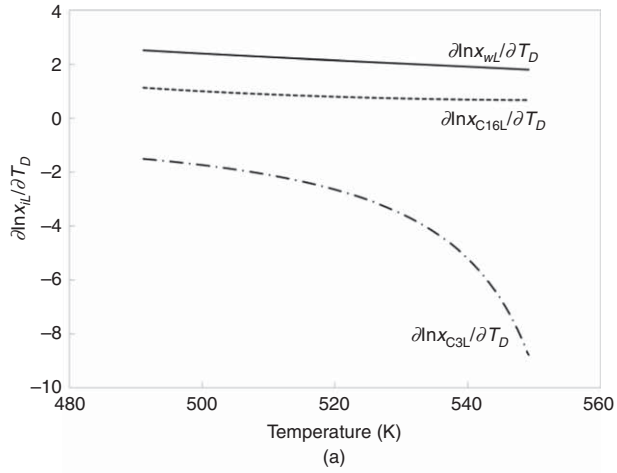

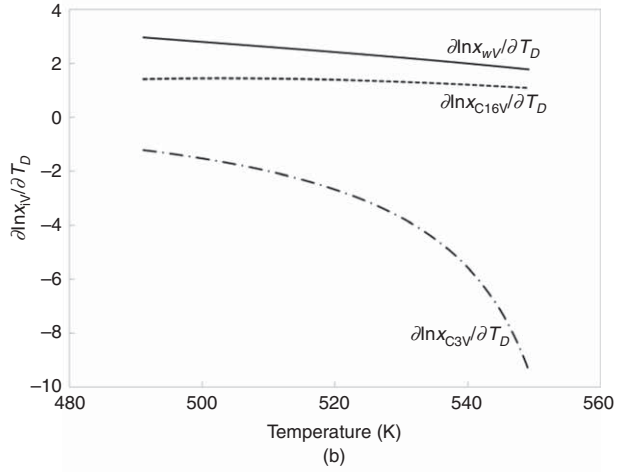

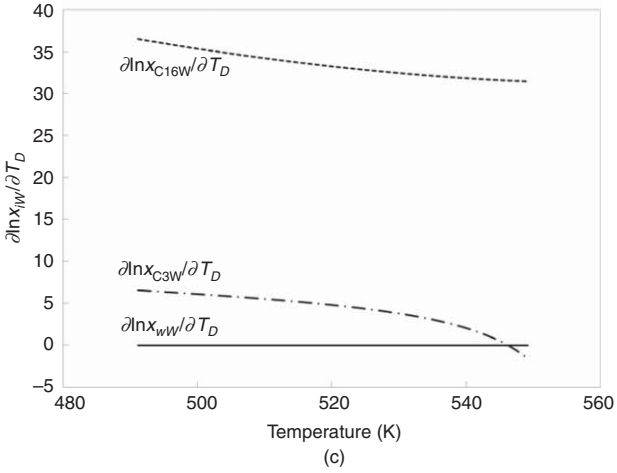

Fig. 4—Sensitivities of the phase compositions to temperature at 80 bar for a mixture of 75% water, 15% C_3, and 10% C_{16} (Case 1). (a) *L* phase, (b) *V* phase, and (c) *W* phase. The properties used for the components are given in Table 1.

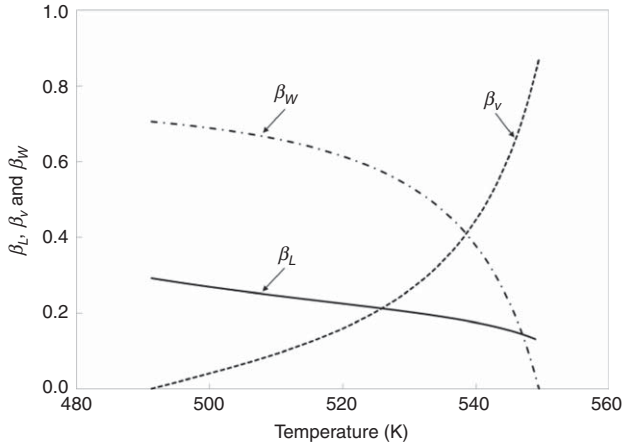

Fig. 5—Mole fractions of the *L*, *V*, and *W* phases in temperature space at 80 bar for a mixture of 75% water, 15% C_3, and 10% C_{16} (Case 1). The properties used for the components are given in Table 1.

composition-temperature space. Because graphical illustration of the Gibbs free energy in composition-temperature space is difficult for more than two components, it is implied by presenting $\ln(x_{ij})$ (associated with the ideal term of the Gibbs free energy). **Fig. 4** shows that the gradients of $\ln(x_{C16})$ and $\ln(x_w)$ with respect to T_D do not change very much in the three-phase region. The derivatives of $\ln(x_{C3})$ decrease with increasing temperature within the three-phase region, especially for the *L* and *V* phases. A similar level of nonlinearity is observed for the fugacity coefficients (associated with the excess term of the Gibbs free energy) within the three-phase region because they are thermodynamic properties dependent on the phase compositions.

The variation of phase compositions (Fig. 3) that is determined by the Gibbs free energy in composition-temperature space results in significant changes in phase mole fractions, β's. **Fig. 5** shows that β_V and β_W become progressively larger and smaller, respectively, as the phase boundary between $L+V+W$ and $L+V$ is approached. Within the three-phase region, β_V increases from 0 to 86%, and β_W decreases from 71 to 0% with increasing temperature. This ternary example showed that narrow-boiling behavior involves rapid changes in the properties and amounts of equilibrium phases with temperature, but the sensitivities depend on how the equilibrium-phase compositions vary relative to the overall composition in temperature space.

Near-Degeneracy of the DS Equations. The DS equations consist of two types of equations, the enthalpy and material-balance equations, which are solved for T_D and β's. Gaussian elimination of the column with $\partial g_{N_P}/\partial T_D$ in the DS Jacobian matrix clearly shows that the matrix tends to be ill-conditioned for narrow-boiling fluids. Then, the limiting singularity of the Jacobian matrix can be easily understood when $\partial g_{N_P}/\partial T_D$ tends to infinity. This subsection presents an example to show the effect of narrow-boiling behavior on the DS Jacobian matrix.

Fig. 6 shows the derivatives of g_1, g_2, and g_3 in the three-phase region for Case 1 (see Fig. 2 for phase boundaries in temperature). Temperature and enthalpies are scaled with $T_{\text{ref}} = 300$ K and $\underline{H}_{\text{spec}} = 15\,000$ J/mol, respectively, in Case 1. The derivatives of g_3 (Eq. 4 with N_P of 3) are greater than those of g_1 and g_2 (Eq. 3 with N_P of 3) by a few orders of magnitude. Also, the derivatives of g_1 and g_2 with respect to T_D exhibit significant sensitivity in the region of narrow-boiling behavior presented in Fig. 2 (at temperatures approximately higher than 534 K).

Fig. 7 presents the condition number of the Jacobian matrix in the three-phase region for Case 1. It increases as temperature increases up to 549.25 K, at which the *W* phase disappears. All calculations in this research use the double-precision floating-point numbers, and the Jacobian matrix with a condition number higher than 10^6 is considered to be ill-conditioned. On this basis, the Jacobian matrix is ill-conditioned at temperatures higher than approximately 534 K in Fig. 7. Fig. 7 also presents that the condition number that is based on one-norms is close to that based on singular value decomposition (SVD) in this case.

To illustrate further the degenerate equations, the Jacobian matrices for Case 1 at two different temperatures, 491.83 and 549.25 K, are factorized with SVD. The higher temperature is in the narrow-boiling region. At 491.83 K, SVD gives

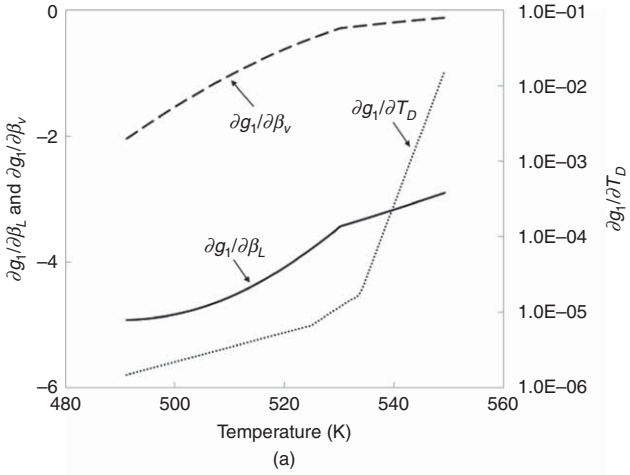

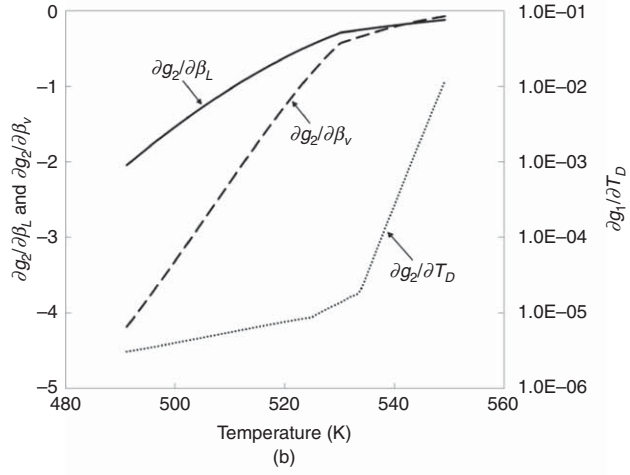

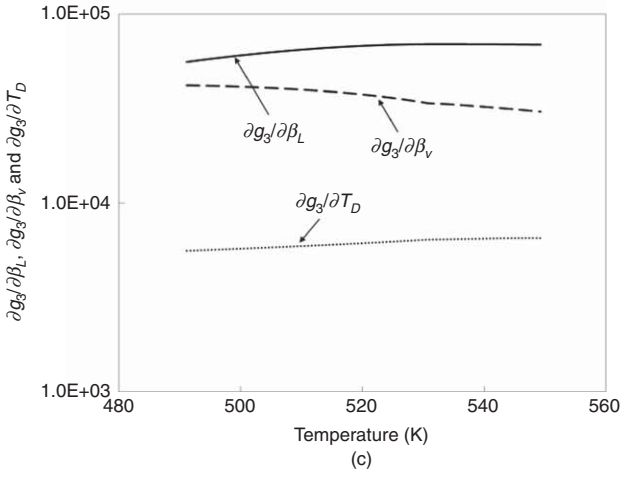

Fig. 6—Elements of the 3×3 Jacobian matrix, at 80 bar for a mixture of 75% water, 15% C_3, and 10% C_{16} (Case 1). The properties used for the components are given in Table 1. (a) Derivatives of g_1, $\partial g_1/\partial \beta_L$, $\partial g_1/\partial \beta_v$, and $\partial g_1/\partial T_D$. The g_1 equation is defined in Eq. 3 with N_P of 3. (b) Derivatives of g_2, $\partial g_2/\partial \beta_L$, $\partial g_2/\partial \beta_v$, and $\partial g_2/\partial T_D$. The g_2 equation is defined in Eq. 3 with N_P of 3. (c) Derivatives of g_3, $\partial g_3/\partial \beta_L$, $\partial g_3/\partial \beta_v$, and $\partial g_3/\partial T_D$. The g_3 equation is defined in Eq. 4 with N_P of 3.

$$\begin{bmatrix} -7.28\times10^{-5} & 0.53 & 0.85 \\ -5.76\times10^{-5} & -0.85 & 0.53 \\ 0.99 & -9.93\times10^{-6} & 9.23\times10^{-5} \end{bmatrix} \begin{bmatrix} 7.04\times10^{4} & 0 & 0 \\ 0 & 2.49 & 0 \\ 0 & 0 & 5.18\times10^{-1} \end{bmatrix} \begin{bmatrix} 0.80 & -0.60 & -0.08 \\ 0.60 & 0.80 & -0.03 \\ -0.08 & 0.02 & -0.99 \end{bmatrix}.$$

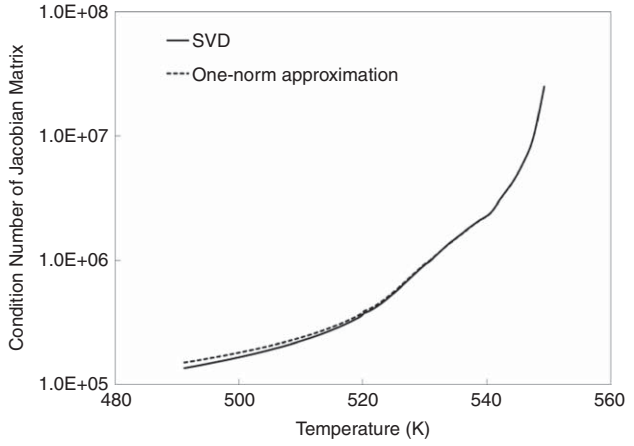

Fig. 7—Condition number of the Jacobian matrix within the three-phase region at 80 bar for a mixture of 75% water, 15% C_3, and 10% C_{16} (Case 1). The properties used for the components are given in Table 1.

At 549.25 K, the Jacobian matrix can be factorized as

$$\begin{bmatrix} -3.55\times10^{-5} & 0.99 & 1.45\times10^{-2} \\ -1.80\times10^{-6} & -1.45\times10^{-2} & 0.99 \\ 0.99 & -3.55\times10^{-5} & 2.31\times10^{-6} \end{bmatrix} \begin{bmatrix} 7.58\times10^{4} & 0 & 0 \\ 0 & 1.09 & 0 \\ 0 & 0 & 3.03\times10^{-3} \end{bmatrix} \begin{bmatrix} 0.91 & -0.41 & 3.41\times10^{-2} \\ 0.40 & 0.89 & -0.22 \\ -0.09 & -0.20 & -0.98 \end{bmatrix}.$$

One can calculate the condition number as the ratio of the maximum singular value to the minimum singular value given in the diagonal matrix. Thus, the condition number is 1.36×10^5 at 491.83 K and 2.50×10^7 at 549.25 K. The corresponding one-norm approximation is 1.52×10^5 at 491.83 K and 2.50×10^7 at 549.25 K.

This example shows that it is no longer appropriate to solve the DS equations simultaneously, when they are nearly degenerate. The DS algorithm presented in this research decouples temperature from the other variables when solving degenerate DS equations. A question as to which conditions the narrow-boiling behavior occurs under in thermal oil recovery merits further investigation. Nevertheless, the DS algorithm presented in the current paper can robustly handle the degeneracy issue that may occur for a variety of reasons, as shown in the next section.

Case Studies

This section shows applications of the direct-substitution (DS) algorithm presented in this paper for three and four phases. For three phases, two mixtures are considered: One is a ternary, and the other is a five-component mixture. The DS algorithm is tested for a number of different pressure-enthalpy (PH) conditions in the three-phase region. The condition numbers of the Jacobian matrices are greater than 10^6 at many of the conditions tested. In the four-phase case, a four-component mixture forms the L_1, L_2, W, and V phases.

Case 1. This case was used to explain the narrow-boiling behavior in the preceding section. The properties of this ternary mixture were presented in Table 1 (see Figs. 1 through 6 for various thermodynamic predictions within the three-phase region).

In this subsection, the DS algorithm is used to solve Case 1 with $T_{ref} = 300$ K, $T^L = 450$ K, $T^U = 650$ K, and $\varepsilon_m = \varepsilon_h = \varepsilon_f = 10^{-10}$.

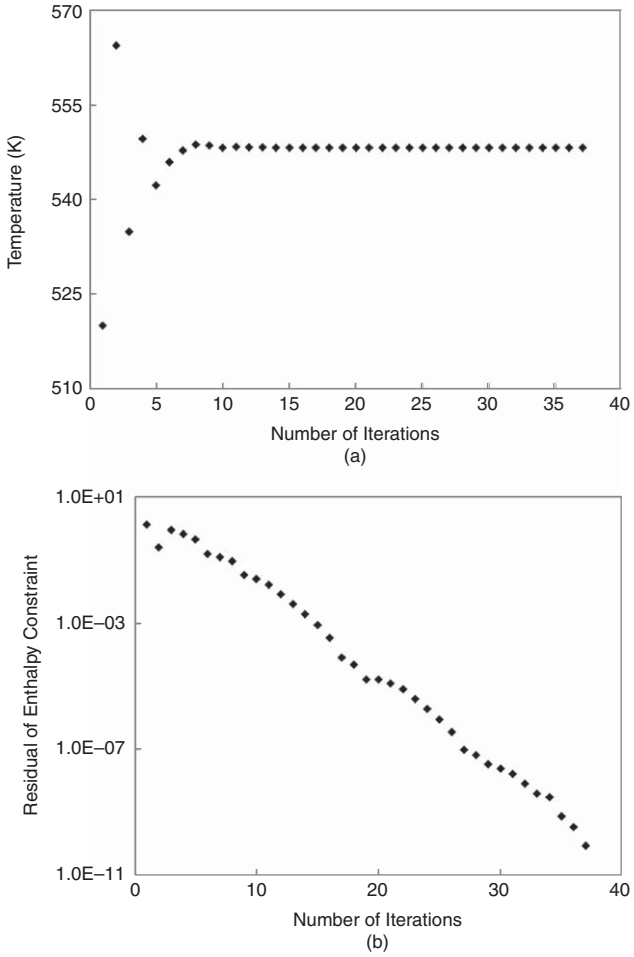

Fig. 8—Convergence behavior of the DS algorithm in PH flash at $P = 80$ bar and $\underline{H}_{spec} = 15\,000$ J/mol for a mixture of 75% water, 15% C_3, and 10% C_{16} (Case 1). The properties used for the components are given in Table 1. The solution temperature is 548.18 K for this PH calculation. (a) Convergence behavior of the DS algorithm in terms of temperature. A high sensitivity of enthalpy to temperature is detected at the third iteration (534.83 K) when the condition number of the Jacobian matrix is 1.48×10^6. The DS algorithm successfully suppresses the temperature oscillation early in the iterative solution. (b) Convergence behavior of the DS algorithm in terms of the enthalpy constraint. The bisection algorithm robustly decreases the g_3 residual at a linear convergence rate.

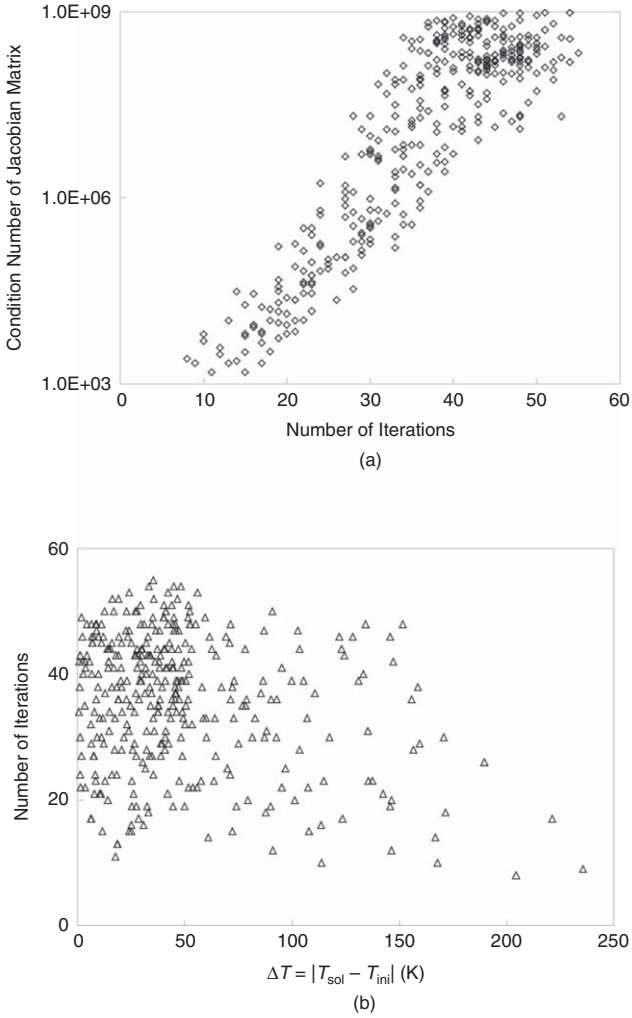

Fig. 9—(a) Number of iterations required for 350 different PH flash calculations in the three-phase region is well-correlated with the condition number of the Jacobian matrix at the converged solution. All the calculations converged to the correct solutions with the DS algorithm presented in this paper. (b) There is no obvious correlation between the number of iterations required and ΔT. The highest deviation of T_{ini} from T_{sol} is 235 K; however, the DS algorithm exhibits no difficulties in these calculations.

A PH flash at 80 bar and 15 000 J/mol results in the solution temperature of 548.18 K. The solution temperature is in the region of the narrow-boiling behavior (see Fig. 2). The initial temperature is set to 520 K. The Newton's iteration step is switched to the bisection algorithm at the third iteration step, when the temperature is 534.83 K with the condition number of 1.48×10^6. The bisection algorithm is used from this iteration step on, until the final convergence is achieved at the 37th iteration step. **Fig. 8** presents the variations of temperature and g_3 during the iterations. It is observed that the DS algorithm successfully suppresses the temperature oscillation early in the iterative solution. The bisection within the DS algorithm robustly decreases the g_3 (Eq. 4 with N_P of 3) residual.

Further testing of the DS algorithm is performed for 350 discrete points in the three-phase region in P-H space. The critical endpoint of type $L = V + W$ is calculated at 131.07 bar and 8393.90 J/mol. These calculations use a fixed initial temperature of 520 K. The algorithm tends to take more iteration steps for the PH specifications in the region of the narrow-boiling behavior. However, all the 350 PH-flash calculations successfully converge to the correct solutions. **Fig. 9** presents that the number of iterations required is correlated with the Jacobian condition number at the converged solution. With the fixed initial temperature, more than 20 iteration steps can be required for the PH specifications at which the condition number is greater than 10^6.

To see the effect of the initial temperature on the convergence behavior, the number of iterations required in the 350 PH flash calculations was also plotted against $\Delta T = |T_{sol} - T_{ini}|$, where T_{sol} is the solution temperature and T_{ini} is the initial temperature, 520 K. As shown in Fig. 9, no correlation was obvious between the number of iterations required and ΔT. The highest deviation of T_{ini} from T_{sol} was 235 K; however, the DS algorithm did not have convergence difficulties in these calculations.

Case 2. Case 2 uses five components used in Luo and Barrufet (2005) as follows: 50% water (w), 15% pseudocomponent 1 (PC1), 10% pseudocomponent 2 (PC2), 10% pseudocomponent 3 (PC3), and 15% pseudocomponent 4 (PC4). The properties of this mixture are given in **Table 2.** Because the binary interaction parameters (BIPs) used by Luo and Barrufet (2005) are unknown, the correlation of Venkatramani and Okuno (2014) is used to assign BIPs for water with the pseudocomponents in this paper. This will result in the underestimation of x_{wL}, as explained in Venkatramani and Okuno (2014). However, these BIP values are

Component	Mole Fraction	MW (g/mol)	T_C (K)	P_C (bar)	ω	C^0_{P1} J/[mol·K]	C^0_{P2} J/[mol·K^2]	C^0_{P3} J/[mol·K^3]	C^0_{P4} J/[mol·K^4]
Water	0.50	18.015	647.300	220.89	0.344	32.20	1.907×10^{-3}	1.055×10^{-5}	-3.596×10^{-9}
PC1	0.15	30.000	305.556	48.82	0.098	–3.50	5.764×10^{-3}	5.090×10^{-7}	0.000
PC2	0.10	156.000	638.889	19.65	0.535	-4.04×10^{-1}	6.572×10^{-4}	5.410×10^{-8}	0.000
PC3	0.10	310.000	788.889	10.20	0.891	–6.10	1.093×10^{-2}	1.410×10^{-6}	0.000
PC4	0.15	400.000	838.889	7.72	1.085	–4.50	8.049×10^{-3}	1.040×10^{-6}	0.000

Binary interaction parameters:

	Water	PC1	PC2	PC3	PC4
Water	0.00000	0.71918	0.45996	0.26773	0.24166
PC1	0.71918	0.00000	0.00000	0.00000	0.00000
PC2	0.45996	0.00000	0.00000	0.00000	0.00000
PC3	0.26773	0.00000	0.00000	0.00000	0.00000
PC4	0.24166	0.00000	0.00000	0.00000	0.00000

MW = molecular weight.

Table 2—Properties for the five-component mixture (Case 2).

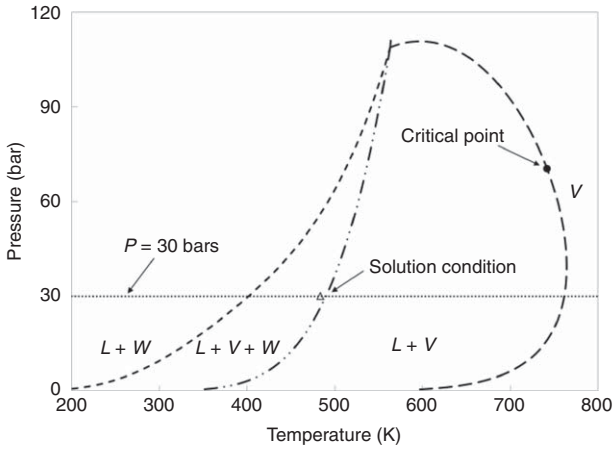

Fig. 10—Phase boundaries in P-T space for the five-component mixture given in Table 2 (Case 2). The critical point is calculated at 741.86 K and 70.50 bar with the Peng-Robinson equation of state.

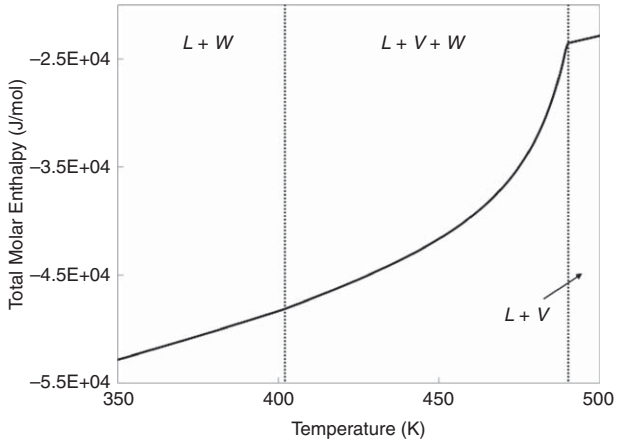

Fig. 11—Total molar enthalpy at 30 bar for the five-component mixture given in Table 2 (Case 2). Three phases are present from 402.01 K to 490.20 K. The total molar enthalpy at 30 bars is sensitive to temperature near the phase boundary between $L+V+W$ and $L+V$.

sufficient for demonstration of the robustness of the DS algorithm for narrow-boiling fluids.

Fig. 10 presents the phase envelope in P-T space. The critical point is calculated at 741.86 K and 70.50 bars. **Fig. 11** shows $\underline{H}^t$ from 350 to 500 K at 30 bar. $\underline{H}^t$ is sensitive to temperature near the phase transition from $L+V+W$ to $L+V$. Three phases are present between 402.01 and 490.20 K at this pressure.

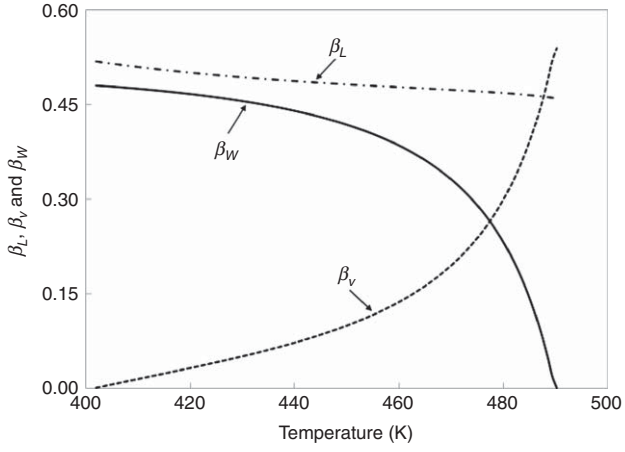

Fig. 12—Mole fractions of the *L*, *V*, and *W* phases at 30 bar for the five-component mixture given in Table 2 (Case 2).

Fig. 12 shows that β_V and β_W are sensitive to temperature in the narrow-boiling region, as in Case 1 (see Fig. 5). The β_V increases from 0 to 54%, and β_W decreases from 48 to 0% as temperature increases within the three-phase region. The sensitivities of β_V and β_W to temperature are attributed to changes of phase compositions with temperature. **Fig. 13** presents components' concentrations in the L and V phases. The W phase always consists of more than 99.99% water within the three-phase region, and its composition is not shown. The L and V phases become richer in water with increasing temperature. The PC1 concentration substantially decreases in the L and V phases with increasing temperature. The other three components in the L and V phases change only slightly with temperature. These variations of phase compositions are analogous to Case 1 presented in Fig. 3. That is, the L-V edge of the tie triangle moves predominantly in the direction parallel to the water-PC1 edge in composition space.

Fig. 14 presents the condition number within the three-phase region at 30 bar. T_{ref} of 300 K and $\underline{H}_{spec}$ of –30 000 J/mol are used to make temperature and enthalpies dimensionless. The condition number significantly increases near the boundary between $L+V+W$ and $L+V$. A PH flash calculation at 30 bar and

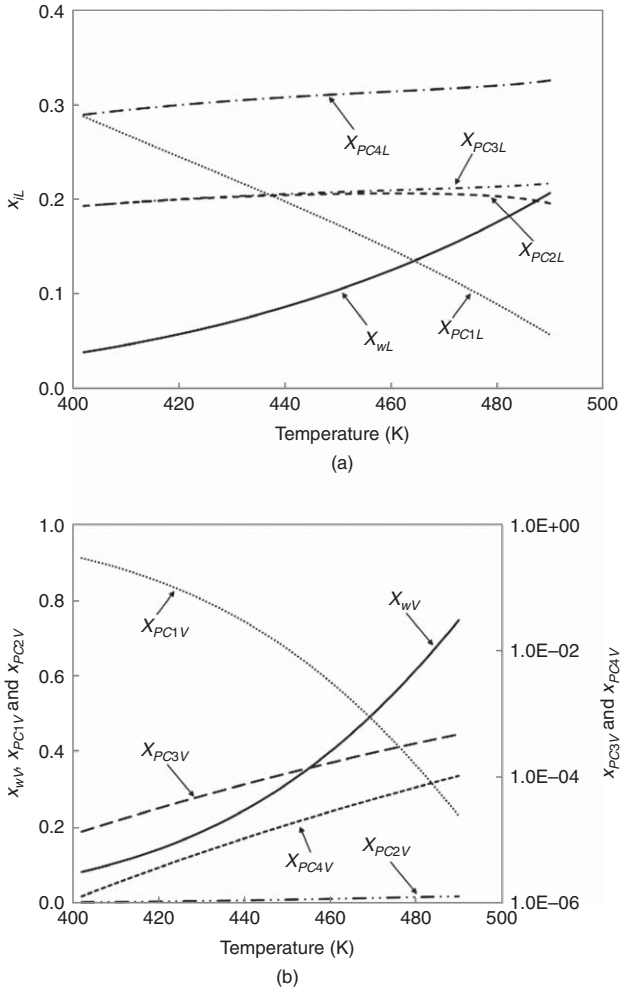

Fig. 13—Concentrations of the components at 30 bar for the five-component mixture given in Table 2 (Case 2); (a) *L* phase and (b) *V* phase. The *W* phase consists of more than 99.99% water within the three-phase region, and its composition is not shown.

–30 000 J/mol is considered for this five-component mixture. The solution temperature is 483.63 K. The initial temperature is set to 450 K. **Fig. 15** shows the convergence behavior of the DS algorithm for this PH flash in terms of T and g_3 (Eq. 4 with N_P of 3). The convergence is achieved at the 26th iteration. The Jacobian condition number is 1.04×10^6 at the third iteration step, and the bisection algorithm robustly solves for T_D based solely on the enthalpy constraint after that.

The critical point for the five-component mixture in P-H space is calculated at 70.50 bar and –3633.99 J/mol. The DS algorithm is tested for 350 discrete P-H conditions in the three-phase region, in which the initial temperature is fixed at 450 K. All the calculations successfully converge to the correct solutions. **Fig. 16** shows that the number of iterations required tends to increase with the condition number of the Jacobian matrix at the convergence. Fig. 16 also shows the sensitivity of the iteration number to $\Delta T = |T_{sol} - T_{ini}|$, where T_{sol} is the solution temperature and T_{ini} is the initial temperature, 450 K. The results show that the convergence behavior of the DS algorithm is insensitive to the initial temperature in these calculations.

Case 3. Case 3 is a four-phase PH flash for a four-component mixture, consisting of 1% water (w), 79% n-C_5 (C_5), 10% n-C_{62} (C_{62}), and 10% n-C_{85} (C_{85}). The properties of this mixture are given in **Table 3.**

The four equilibrium phases in this case are the L_1, L_2, V, and W phases. As mentioned in the DS algorithm section, K-value

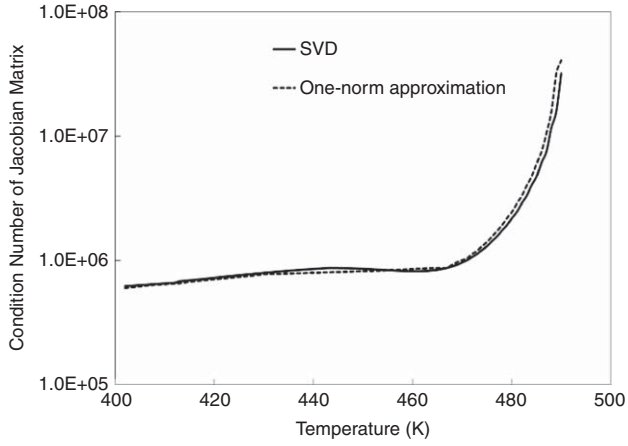

Fig. 14—Condition number of the Jacobian matrix within the three-phase region at 30 bar for the five-component mixture given in Table 2 (Case 2).

estimates for four phases can be given by the method presented in this research and a certain K-value set for L_1 and L_2. To our knowledge, however, there is no established K-value correlation for hydrocarbon liquid phases in the literature. This is a major technical issue to be resolved in this research area, but beyond the scope of the current paper.

In this case study, therefore, x_{iL1} and x_{iL2} specific to this fluid system were correlated with temperature as follows: $x_{C5L1} = -2.1567 \times 10^{-2}\, T + 11.1825$, $x_{C62L1} = 2.0825 \times 10^{-2}\, T - 9.8330$, $x_{C85L1} = 4.1415 \times 10^{-4}\, T - 1.9527 \times 10^{-1}$, $x_{C5L2} = -1.5333 \times 10^{-2}\, T + 8.2043$, $x_{C62L2} = 2.2374 \times 10^{-2}\, T - 10.5615$, and $x_{C85L2} = -7.3442 \times 10^{-3}\, T + 3.4986$. The hydrocarbon concentrations in the W phase (x_{hcW}) were set to 10^{-8}. Then, Eq. 8 was used for L_1 and L_2 by replacing L in the equation with L_1 and L_2, respectively. Note that these correlations were made only to demonstrate four-phase PH flash with the current DS algorithm.

Fig. 17 shows $\underline{H}^t$ from 460 K to 480 K at 36 bars. Four phases are present between 473.37 K and 473.62 K at this pressure. $\underline{H}^t$ is sensitive to temperature in the entire four-phase region. **Fig. 18** presents the condition numbers of the 4×4 Jacobian matrix within the four-phase region at 36 bar by use of SVD and the one-norm approximation. Temperature and enthalpy are made dimensionless by T_{ref} of 300 K and $\underline{H}_{spec}$ of 67 500 J/mol. The condition number from the one-norm approximation is in reasonable agreement with that from SVD. The condition numbers presented are larger than 10^6 because the entire four-phase region is narrow-boiling (see Fig. 17).

A PH flash calculation at 36 bar and 67 500 J/mol is considered for this quaternary mixture. The solution temperature is 473.51 K. The initial temperature is set to 460 K, which is in the L_1-L_2 two-phase region. **Fig. 19** shows the convergence behavior of the DS algorithm for this PH specification in terms of T and g_4 (the enthalpy constraint, Eq. 4, with N_P of 4). The convergence is achieved at the 38th iteration. The Jacobian condition number is calculated to be 3.50×10^8 with the one-norm approximation at the 14th iteration step, and the bisection algorithm robustly solves for T_D solely on the basis of the enthalpy constraint from this iteration step on.

Discussion

This section is to address unanswered questions regarding isenthalpic (PH) flash with the direct-substitution (DS) algorithm. The first question is whether the DS algorithm can handle the limiting narrow-boiling behavior with one degree of freedom. The second question is how the scaling of variables affects the convergence behavior of the DS algorithm.

One Degree of Freedom. The preceding section demonstrated the robustness of the proposed DS algorithm for narrow-boiling

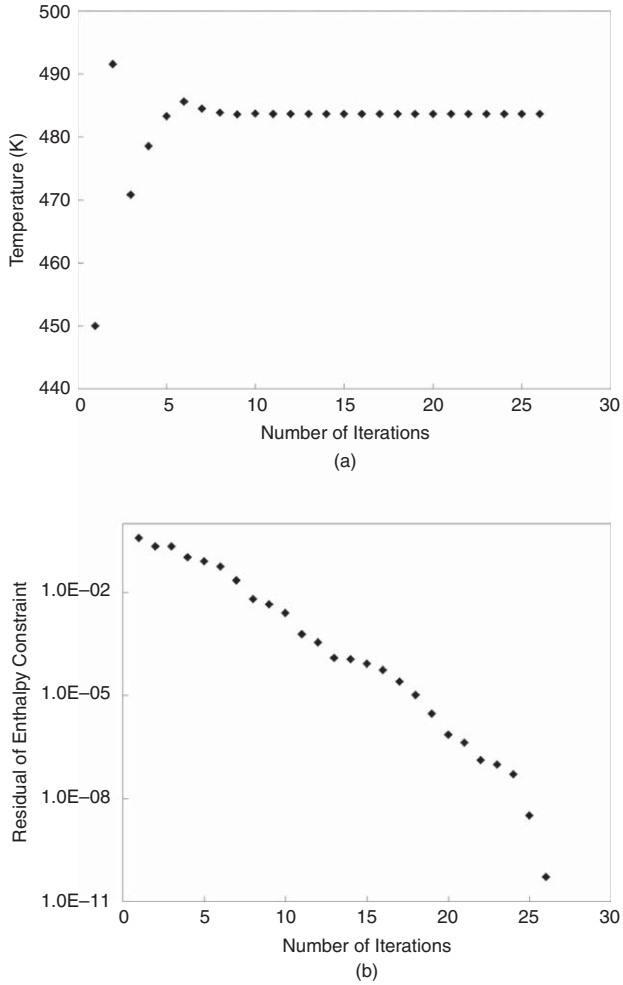

Fig. 15—Convergence behavior of the DS algorithm in PH flash at $P = 30$ bar and $H_{spec} = -30\,000$ J/mol for the five-component mixture given in Table 2 (Case 2). The solution temperature is 483.63 K for this PH flash. (a) Convergence behavior of the DS algorithm in terms of temperature. A high sensitivity of enthalpy to temperature is detected at the third iteration (470.80 K) when the condition number of the Jacobian matrix is 1.04×10^6. The DS algorithm successfully suppresses the temperature oscillation early in the iterative solution. (b) Convergence behavior of the DS algorithm in terms of the enthalpy constraint. The bisection algorithm robustly decreases the g_3 residual at a linear convergence rate.

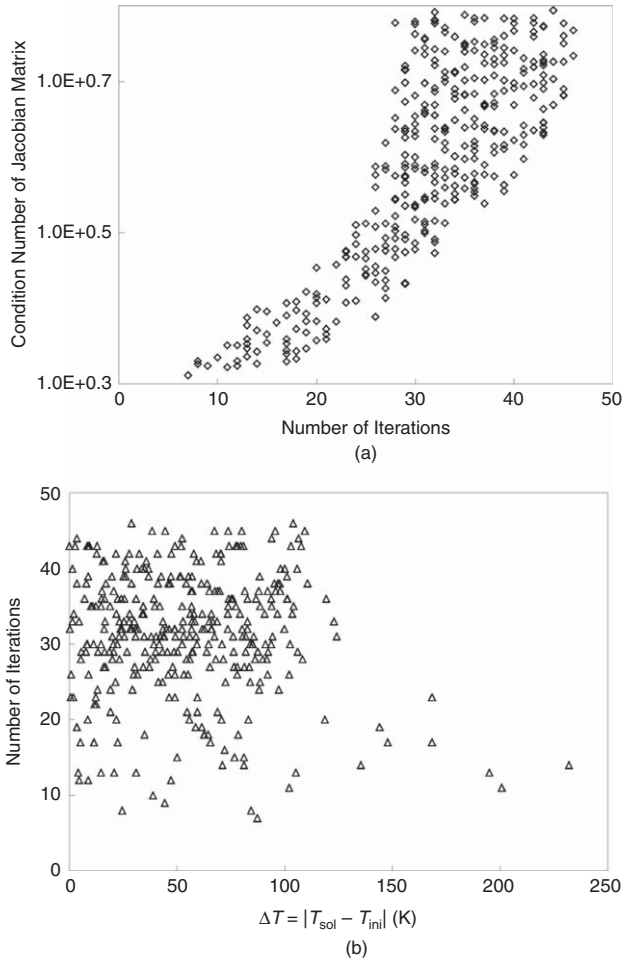

Fig. 16—(a) Number of iterations required for 350 different PH flash calculations in the three-phase region is correlated to the condition number of the Jacobian matrix at the converged solution. All the calculations converged to the correct solutions with the DS algorithm presented in this paper. (b) The highest deviation of T_{ini} from T_{sol} is 230 K; however, the convergence behavior of the DS algorithm is insensitive to the initial temperature in these calculations.

behavior for a fixed number of phases [i.e., three and four phases in this paper and two phases in Zhu and Okuno (2014)]. As mentioned in the Introduction, one degree of freedom is the limiting case of narrow-boiling behavior, in which the total molar enthalpy is discontinuous in temperature. Because the DS algorithm assumes a certain number of equilibrium phases, misidentification

Component	Mole Fraction	MW (g/mol)	T_C (K)	P_C (bar)	ω	C^0_{P1} J/[mol·K]	C^0_{P2} J/[mol·K^2]	C^0_{P3} J/[mol·K^3]	C^0_{P4} J/[mol·K^4]
Water	0.01	18.015	647.300	220.89	0.344	32.20	1.907×10^{-3}	1.055×10^{-5}	-3.596×10^{-9}
C_5	0.79	72.151	469.600	33.74	0.251	–3.63	4.873×10^{-1}	-2.580×10^{-4}	5.305×10^{-8}
C_{62}	0.10	864.000	983.204	15.46	0.646	3.28×10	4.933	-1.956×10^{-3}	0.000
C_{85}	0.10	1186.000	1034.525	14.89	0.668	4.57×10	6.794	-2.684×10^{-3}	0.000

Binary interaction parameters:

	Water	C_5	C_{62}	C_{85}
Water	0.000	0.619	0.242	0.242
C_5	0.619	0.000	0.080	0.070
C_{62}	0.242	0.080	0.000	0.000
C_{85}	0.242	0.070	0.000	0.000

MW = molecular weight.

Table 3—Properties for the quaternary mixture (Case 3).

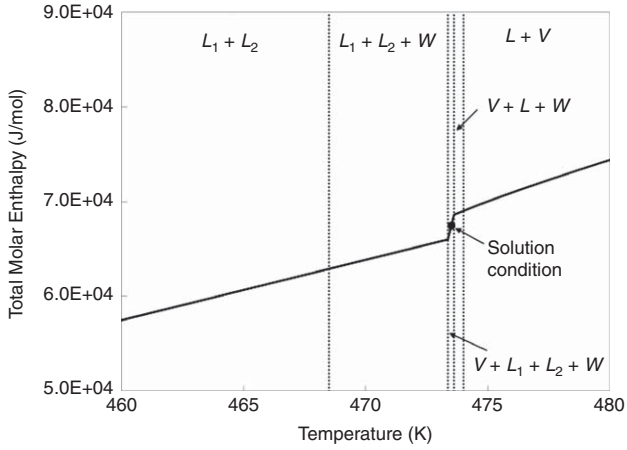

Fig. 17—Total molar enthalpy at 36 bar for the quaternary mixture given in Table 3 (Case 3). Four phases are present from 473.37 to 473.62 K. The total molar enthalpy at 36 bar is sensitive to temperature in the entire four-phase region.

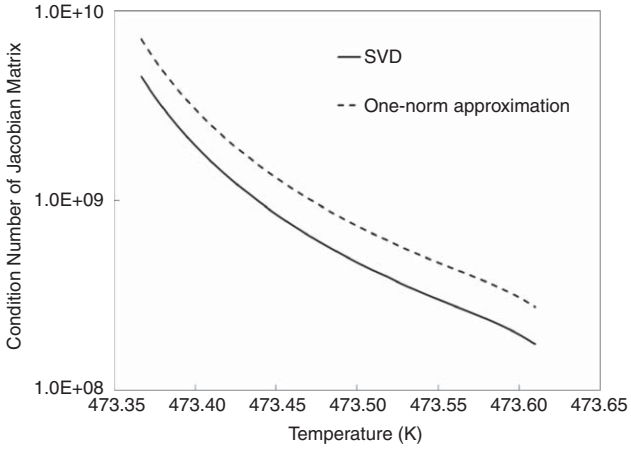

Fig. 18—Condition number of the Jacobian matrix within the four-phase region at 36 bars for the quaternary mixture given in Table 3 (Case 3).

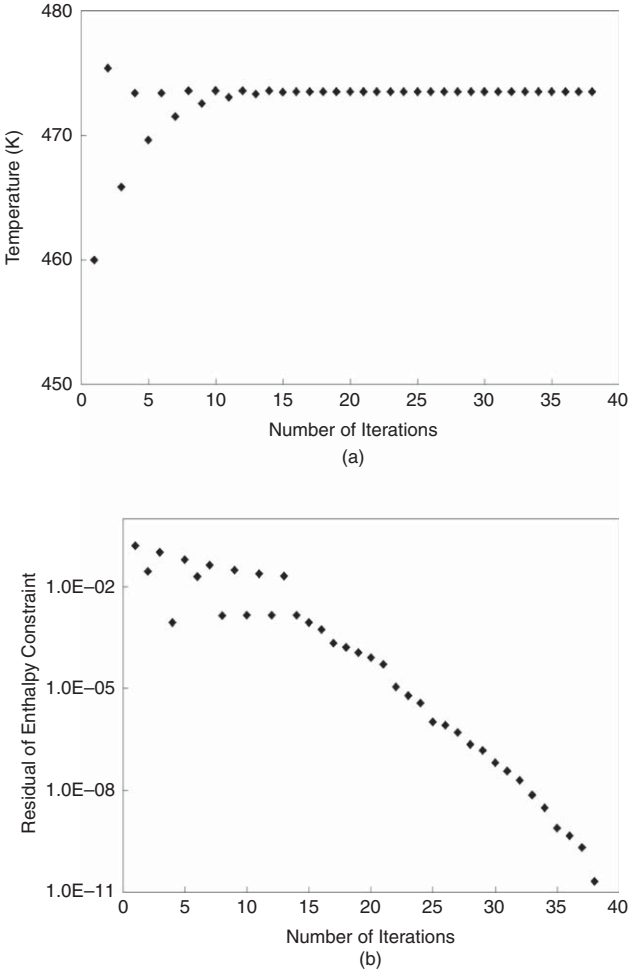

Fig. 19—Convergence behavior of the DS algorithm in PH flash at $P = 36$ bar and $\underline{H}_{spec} = 67\,500$ J/mol for the quaternary mixture given in Table 3 (Case 3). The solution temperature is 473.51 K for this PH flash. (a) Convergence behavior of the DS algorithm in terms of temperature. A high sensitivity of enthalpy to temperature is detected at the 14th iteration (473.59 K) when the condition number of the Jacobian matrix is 3.50×10^8. The DS algorithm successfully suppresses the temperature oscillation early in the iterative solution. (b) Convergence behavior of the DS algorithm in terms of the enthalpy constraint. The bisection algorithm robustly decreases the residual of enthalpy constraint at a linear convergence rate.

of the phase number can occur when the PH-flash solution has only one degree of freedom. This subsection is to show how the DS algorithm can robustly handle the limiting narrow-boiling behavior, which has not been given in the literature.

The equimolar mixture of water and n-C_5 is considered. Their properties are given in Table 3 as part of the fluid used for Case 3. **Fig. 20** presents the T-x diagram for this binary at 10 bar on the basis of the Peng-Robinson (PR) equation of state (EOS). Three equilibrium phases, L, V, and W, are calculated to coexist at 388.32 K (T_{3P}). The equimolar mixture exhibits the phase transition between $L + W$ and $V + W$ through the three-phase coexistence at T_{3P}, in which the degree of freedom is one.

Fig. 21 presents $\underline{H}^I$ from 350 to 500 K at 10 bar and the limiting nonlinearity of $\underline{H}^I$ with respect to temperature as a discontinuity. When the solution is at T_{3P}, the two-phase PH flash results in temperature oscillations. The oscillation occurs in a quite regular manner because the non-W phase changes between V and L discontinuously on the phase transition at T_{3P}, as one can clearly see in Fig. 20.

The simple remedy proposed here is to split the oscillating phase into two phases of initially equal amounts and compositions

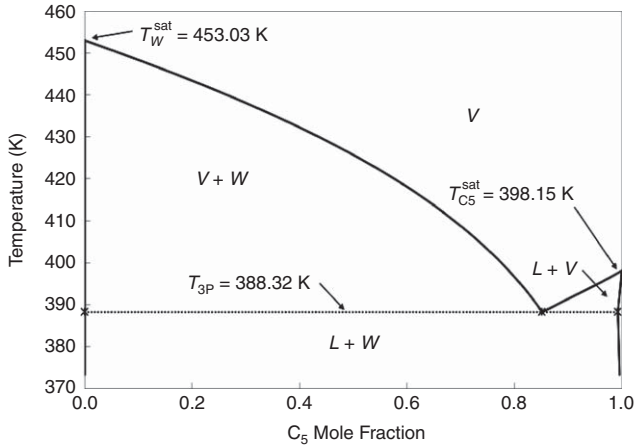

Fig. 20—T-x diagram for the equimolar mixture of water/n-C_5 at 10 bar on the basis of the PR EOS. The properties used for the components are given in Table 3 as part of the fluid used for Case 3. Three equilibrium phases, L, V, and W, are calculated to coexist at 388.32 K (T_{3P}). The saturation temperatures of water and C_5 are 453.03 and 398.15 K, respectively, at 10 bar. The equimolar mixture exhibits the phase transition between $L + W$ and $V + W$ through the three-phase coexistence at T_{3P}, in which the degree of freedom is 1.

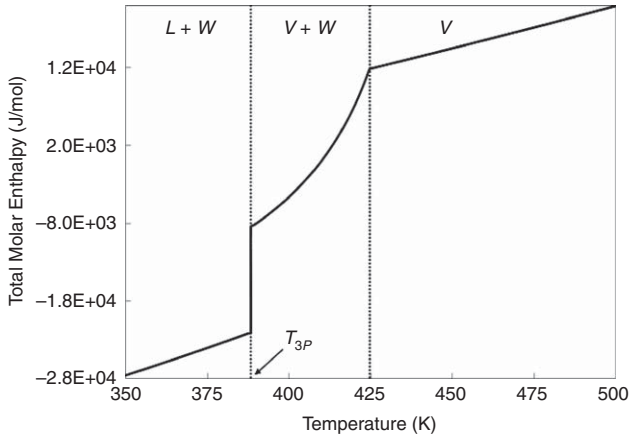

Fig. 21—Total molar enthalpy for the equimolar mixture of water/*n*-C_5 at 10 bar. The properties used for the components are given in Table 3 as part of the fluid used for Case 3. The limiting nonlinearity of $\underline{H}^t$ with respect to temperature as a discontinuity occurs at T_{3P}.

only for the first time the oscillation is detected. Their K values for this and the subsequent iterations are then estimated directly on the basis of the oscillating phase compositions (i.e., L and V in Fig. 20). After that, the system of the DS equations, which is now 3×3 after the addition of a phase, is solved for temperature and phase mole fractions until a convergence is achieved. Thus, Steps 9 through 15 given in this paper are repeated until the convergence. This new remedy can provide good K-value estimates for one degree of freedom on the basis of the mechanistic understanding of the reason for the temperature oscillation.

The new remedy with the two- and three-phase DS algorithms developed in this research was applied to the PH flash calculation of the binary mixture at 10 bar and –15 000 J/mol, which had the solution at T_{3P}. The initial temperature was set to 370 K, which was in the *L*-*W* two-phase region (see Figs. 20 and 21). **Fig. 22** shows the resulting convergence behavior in terms of T and the enthalpy residual. With the procedure given in Zhu and Okuno (2014), the temperature oscillation was detected at the 14th iteration step when temperature was 388.21 K. The convergence was achieved at the 26th iteration by use of the new remedy.

The proposed remedy is different from that of Michelsen (1987) in the way of estimating K values after splitting an oscillating phase. Michelsen (1987) also suggested splitting the oscillating phase into two phases of initially equal amounts and compositions. In his remedy, however, the maximum compressibility factor was chosen for one of the split phases and the minimum for the other, and K values were estimated on the basis of the ratios of fugacity coefficients. As shown in Zhu and Okuno (2014), this approach does not resolve the convergence issues associated with narrow-boiling behavior when only one root exists in the solution of a cubic EOS for an oscillating phase. This is because K values for the split two phases become unity for such a case, resulting in a singular Jacobian matrix in the DS algorithm.

The DS algorithm of Michelsen (1987) was applied for PH flash of this binary mixture, as implemented by Zhu and Okuno (2014). However, it stopped from proceeding at the 14th iteration step because of the singularity, as mentioned previously.

The issue with one degree of freedom arises as part of the more general problem that the number of equilibrium phases is unknown in temperature and composition space in PH flash. A potential way is to perform flash and stability analysis simultaneously, as originally proposed by Gupta et al. (1991). However, the PH stability analysis is beyond the scope of the current paper, and will be addressed in future publications.

Scaling of Variables. A large condition number of the Jacobian matrix is used as the indicator for narrow-boiling behavior in the

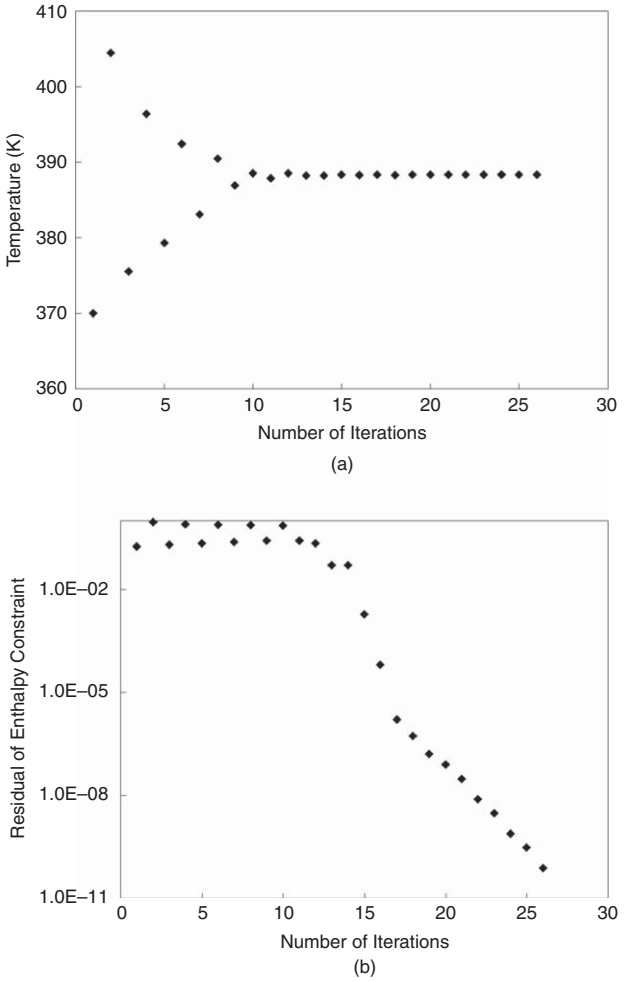

Fig. 22—Convergence behavior of the DS algorithm with the new remedy in PH flash at $P = 10$ bar and $\underline{H}_{spec} = -15\,000$ J/mol for the equimolar mixture of water/*n*-C_5. The properties used for the components are given in Table 3 as part of the fluid used for Case 3. The solution temperature is 388.32 K for this PH calculation. (a) Convergence behavior of the DS algorithm with the new remedy in terms of temperature. With the procedure given in Zhu and Okuno (2014), the temperature oscillation is detected at the 14th iteration step when temperature is 388.21 K. (b) Convergence behavior of the DS algorithm with the new remedy in terms of the enthalpy constraint. The convergence is achieved at the 26th iteration by use of the new remedy.

current DS algorithm with dimensionless temperature and enthalpy, T_D and $\underline{H}_D$. When the variables are dimensional as in some of the PH flash algorithms presented in the literature, the Jacobian condition number depends on the units used. Although the condition number can be made lower by use of different units, this does not solve the convergence issue associated with narrow-boiling fluids. This is illustrated with the fluid used for Case 1.

Fig. 23 shows the condition numbers of the Jacobian matrix with different units for Case 1. With temperature in K and enthalpy in either J/mol or kJ/mol, the Jacobian matrix is ill-conditioned within the entire three-phase region. With temperature in K and enthalpy in MJ/mol, the condition number of the Jacobian matrix is lower than 10^6 for temperatures lower than 518.27 K. With temperature in K and enthalpy in GJ/mol, the Jacobian matrix is well-conditioned within the entire three-phase region. However, Fig. 2 clearly shows that narrow-boiling behavior physically exists within the three-phase region near the high-temperature boundary, regardless of the units used in the computations.

The convergence behavior of the DS algorithm for Case 1 with dimensionless variables was previously shown in Fig. 8. With temperature in K and enthalpy in J/mol, kJ/mol, or MJ/mol, the convergence behavior is the same as in Fig. 8. This is because the

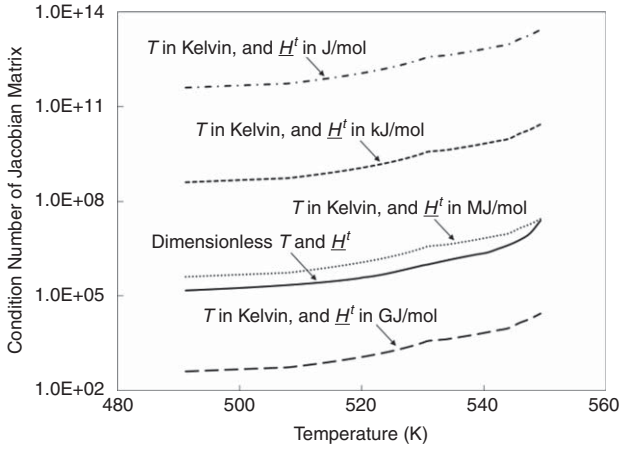

Fig. 23—Condition numbers of the Jacobian matrix within the three-phase region at 80 bar for a mixture of 75% water, 15% C_3, and 10% C_{16} (Case 1). The properties used for the components are given in Table 1. With temperature in K and enthalpy in either J/mol or kJ/mol, the Jacobian matrix is ill-conditioned within the entire three-phase region. With temperature in K and enthalpy in MJ/mol, the condition number of the Jacobian matrix is lower than 10^6 for temperatures lower than 518.27 K. With temperature in K and enthalpy in GJ/mol, the Jacobian matrix is well-conditioned within the entire three-phase region. However, Fig. 2 clearly shows that narrow-boiling behavior physically exists within the three-phase region near the high-temperature boundary, regardless of the units used in the computations.

algorithm switches from the Newton's iteration step to the bisection algorithm at the third iteration with these selections of units.

With temperature in K and enthalpy in GJ/mol, the DS algorithm attempts to use only Newton's steps because the Jacobian condition number is made lower than 10^6 in the entire three-phase region. Then, the DS algorithm exhibits oscillations because the bisection algorithm is never used even in the narrow-boiling region between 533.64 and 549.25 K. Thus, the robustness of the DS algorithm can be affected by the selection of units when dimensional variables are used. It is recommended that the variables be made dimensionless in PH flash.

Conclusions

This paper presented a robust algorithm for multiphase PH flash that can be applied to practical engineering problems (i.e., water-containing hydrocarbon mixtures involving narrow-boiling phases). A new method was also presented for K-value estimates for three phases for water-containing hydrocarbon mixtures, which can be extended to four phases. A number of isenthalpic (PH) flash calculations performed in the case studies demonstrated the robustness of the multiphase direct-substitution (DS) algorithm. Conclusions are as follows:

- Narrow-boiling behavior is characterized by rapid changes in the properties and amounts of equilibrium phases with a small change in temperature. One degree of freedom is the limiting case of narrow-boiling, in which the total enthalpy is discontinuous in temperature. The DS equations tend to be degenerate for narrow-boiling fluids; the DS Jacobian matrix becomes singular with one degree of freedom. Further investigation is necessary for the systematic understanding of thermodynamic conditions under which narrow-boiling behavior occurs. Nevertheless, the adaptive Newton-bisection approach presented can robustly handle the degeneracy issue that may occur for a variety of reasons.
- PH flash for systems with one degree of freedom causes the DS algorithm to exhibit temperature oscillation. Such temperature oscillation occurs because of a discontinuous phase transition in composition space at the solution temperature, in which the degree of freedom is one. Thus, misidentification of the number of phases should be corrected by adding a phase once the temperature oscillation is detected. The new remedy presented in this paper can robustly handle such cases on the basis of the mechanistic understanding of the reason for the temperature oscillation.
- Superficial reduction of the Jacobian condition number with different unit systems does not improve the convergence issues associated with narrow-boiling behavior. Dimensionless temperature and enthalpy should be used in the developed DS algorithm so that the Jacobian condition number can properly identify narrow-boiling behavior.
- The developed DS algorithm exhibited no convergence issue for 350 different PH flash calculations for a ternary mixture, and 350 different PH flash calculations for a five-component mixture. The algorithm was also successfully applied to four phases consisting of the L_1, L_2, V, and W phases. The number of iterations required tends to increase as the condition number of the Jacobian matrix at the converged solution increases, but is insensitive to the initial temperature. It is necessary to test the robustness of the algorithm further with practical thermodynamic conditions encountered in thermal compositional flow simulations.

Nomenclature

A = dimensionless attraction parameter for a Peng-Robinson equation of state (EOS)
B = dimensionless covolume parameter for a cubic EOS
C_{Pj} = heat capacity of phase j
$C^0_{P_i}$ = coefficients of component i defined in Eq. B-6
$\vec{f}$ = vector consisting of N_C residuals of the fugacity equations
f_{ij} = residual of the fugacity equations defined in Eq. 1
g_j = residuals of the material-balance equations (j = 1, 2, …, $N_P - 1$)
g_{NP} = residual of the enthalpy constraint
H = enthalpy
$\underline{H}$ = molar enthalpy
$\underline{J}$ = Jacobian matrix
$\vec{K}$ = vector consisting of N_C K value
K_{ij} = K values of component i in phase j
N_C = number of components
N_P = number of phases
P = pressure
P_c = critical pressure
R = universal gas constant
$\underline{S}$ = molar entropy
t_i = parameter defined in Eq. 3
T = temperature
Tc = critical temperature
x_{ij} = mole fraction of component i in phase j
z_i = mole fraction of component i in a mixture
Z_j = compressibility factor of phase j
β_j = mole fraction of phase j
ε = convergence criterion (e.g., 10^{-10})
φ_{ij} = fugacity coefficient of component i in phase j
ω = acentric factor

Subscripts

$3P$ = three phases
C = critical property
D = dimensionless property
f = fugacity equations
h = enthalpy constraint
hc = hydrocarbon component
i = component index
ini = initial condition
j = phase index
L = oleic phase in three-phase notation
L_1 = oleic phase in four-phase notation
L_2 = solvent-rich liquid phase in four-phase notation
m = mixture or material balance
ref = reference value
sol = solution condition

spec = specified value
w = water component
V = vapor phase
W = aqueous phase

Superscripts

k = index for iteration steps
L = lower bound
sat = saturation temperature
t = total property
T = transpose
U = upper bound
vap = vapor pressure

Acknowledgments

This research was funded by research grants from the Natural Sciences and Engineering Research Council of Canada (RGPIN 418266) and Japan Petroleum Exploration Co. Limited. Di Zhu also received financial support from the China Scholarship Council. Ryosuke Okuno was awarded the SPE Petroleum Engineering Junior Faculty Research Initiation Fellowship. We gratefully acknowledge this support.

References

Agarwal, R.K., Li, Y.K. Nghiem, L.X. et al. 1991. Multiphase Multicomponent Isenthalpic Flash Calculations. *J Can Pet Technol* **30** (3): 69–75. SPE-91-03-07-PA. http://dx.doi.org/10.2118/91-03-07-PA.

Amani, M.J., Gray, M.R. and Shaw, J.M. 2013a. Phase Behavior of Athabasca Bitumen + Water Mixtures at High Temperature and Pressure. *J. Supercritical Fluids* **77:** 142–152. http://dx.doi.org/10.1016/j.supflu.2013.03.007.

Amani, M.J., Gray, M.R. and Shaw, J.M. 2013b. Volume of Mixing and Solubility of Water in Athabasca Bitumen at High Temperature and Pressure. *Fluid Phase Equilibria* **358:** 203–211. http://dx.doi.org/10.1016/j.fluid.2013.07.021.

Brantferger, K.M. 1991. *Development of a Thermodynamically Consistent, Fully Implicit, Compositional, Equation-of-State, Steamflood Simulator*. PhD dissertation, the University of Texas at Austin, Austin, Texas (May 1991).

Brantferger, K.M., Pope, G.A., and Sepehrnoori, K. 1991. Development of a Thermodynamically Consistent, Fully Implicit, Equation-of-State, Compositional Steamflood Simulator. Paper presented at the SPE Symposium on Reservoir Simulation, Anaheim, California, 17–20 February. SPE-21253-MS. http://dx.doi.org/10.2118/21253#MS.

Bruining, J. and Marchesin, D. 2007. Maximal Oil Recovery by Simultaneous Condensation Alkane and Steam. *Physical Review E—Statistical, Nonlinear, and Soft Matter Physics* **75** (3): 036312-1–036312-16. http://dx.doi.org/10.1103/PhysRevE.75.036312.

Butler, R.M. 1991. *Thermal Recovery of Oil and Bitumen*. New Jersey: Prentice Hall.

Chien, M.C.H., Yardumian, H.E., Chung, E.Y. et al. 1989. The Formulation of a Thermal Simulation Model in a Vectorized, General Purpose Reservoir Simulator. Paper presented at the SPE Symposium on Reservoir Simulation, Houston, Texas, 6–8 February. SPE-18418-MS. http://dx.doi.org/10.2118/18418-MS.

Computer Modelling Group (CMG) Ltd. *STARS User Manual*. Version 2011. Calgary, Alberta, Canada.

Economou, I.G., Heidman, J.L., Tsonopoulos, C. et al. 1997. Mutual Solubilities of Hydrocarbons and Water: III. 1-Hexene, 1-Octene, C_{10}–C_{12} Hydrocarbons. *AIChE J*. **43** (2): 535–546. http://dx.doi.org/10.1002/aic.690430226.

Eubank, P.T., Wu, C.H., Alvarado, J.F. et al. 1994. Measurement and Prediction of Three-Phase Water/Hydrocarbon Equilibria. *Fluid Phase Equilibria* **102** (2): 181–203. http://dx.doi.org/10.1016/0378-3812(94)87076-4.

Glandt, C.A. and Chapman, W.G. 1995. Effect of Water Dissolution on Oil Viscosity. *SPE Res Eval & Eng* **10** (1): 59–64. SPE-24631-PA. http://dx.doi.org/10.2118/24631-PA.

Grabowski, J.W., Vinsome, P.K., Lin, R.C. et al. 1979. A Fully Implicit General Purpose Finite-Difference Thermal Model for In Situ Combustion and Steam. Paper presented at the SPE Annual Technical Conference and Exhibition, Las Vegas, Nevada, 23–26 September. SPE-8396 -MS. http://dx.doi.org/10.2118/8396-MS.

Griswold, J. and Kasch, J.E. 1942. Hydrocarbon-Water Solubilities at Elevated Temperatures and Pressures. *Industrial and Engineering Chemistry* **34** (7): 804–806. http://dx.doi.org/10.1021/ie50391a007.

Gupta, A.K., Bishnoi, P.R., and Kalogerakis, N. 1990. Simultaneous Multiphase Isothermal/Isenthalpic Flash and Stability Calculations for Reacting/Non-Reacting Systems. *Gas Separation and Purification* **4:** 215–222. http://dx.doi.org/10.1016/0950-4214(90)80045-M.

Gupta, A.K., Bishnoi, P.R., and Kalogerakis, N. 1991. A Method for the Simultaneous Phase Equilibria and Stability Calculations for Multiphase Reacting and Non-Reacting Systems. *Fluid Phase Equilibria* **63** (1): 65–89. http://dx.doi.org/10.1016/0378-3812(91)80021-M.

Hagoort, J., Leijnse, A., and van Poelgeesi F. 1976. Steam-Strip Drive: A Potential Tertiary Recovery Process. *J Pet Technol* **28** (12): 1409–1419. SPE-5570-PA. http://dx.doi.org/10.2118/5570-PA.

Heidman, J.L., Tsonopoulos, C., Brady, C.J. et al. 1985. High-Temperature Mutual Solubilities of Hydrocarbons and Water. Part II: Ethylbenzene, Ethylcyclohexane, and *n*-Octane. *AIChE J*. **31** (3): 376–384. http://dx.doi.org/10.1002/aic.690310304.

Iranshahr, A., Voskov, D.V., and Tchelepi, H.A. 2010. Tie-Simplex Parameterization for EOS-Based Thermal Compositional Simulation. *SPE J*. **15** (2): 545–556. SPE-119166 -PA. http://dx.doi.org/10.2118/119166-PA.

Ishimoto, K., Pope, G.A., and Sepehrnoori, K. 1987. An Equation of State Steam Simulator. *In Situ* **11** (1): 1–37.

Jha, R.K., Kumar, M., Benson, I. et al. 2013. New Insights Into Steam/Solvent-Coinjection-Process Mechanism. *SPE J*. **18** (5): 867–877. SPE-159277-PA. http://dx.doi.org/10.2118/159277-PA.

Keshavarz, M., Okuno, R., and Babadagli, T. 2014a. Effcient Oil Displacement Near the Chamber Edge in ES-SAGD. *J. Petrol. Sci. & Eng*. **118:** 99–113. http://dx.doi.org/10.1016/j.petrol.2014.04.007.

Keshavarz, M., Okuno, R., and Babadagli, T. 2014b. Optimal Application Conditions for Steam-Solvent Coinjection. *SPE Res Eval & Eng* **18** (1): 20–38. SPE-165471-PA. http://dx.doi.org/10.2118/165471-PA.

Kesler, M.G. and Lee, B.I. 1976. Improve Prediction of Enthalpy of Fractions. *Hydrocarbon Processing* **55** (3): 153–158.

Liu, K., Subramanian, G., Dratler, D.I. et al. 2009. A General Unstructured-Grid, Equation-of-State-Based, Fully Implicit Thermal Simulator for Complex Reservoir Processes. *SPE J*. **14** (2): 355–361. SPE-106073-PA. http://dx.doi.org/10.2118/106073-PA.

Luo, S. and Barrufet, M.A. 2005. Reservoir Simulation Study of Water-in-Oil Solubility Effect on Oil Recovery in Steam Injection Process. *SPE Res Eval Eng* **8** (6): 528–533. SPE-89407-PA. http://dx.doi.org/10.2118/89407-PA.

McGarry, J. 1983. Correlation and Prediction of the Vapor Pressures of Pure Liquids Over Large Pressure Ranges. *Industrial and Engineering Chemistry Process Design and Development* **22** (2): 313–322. http://dx.doi.org/10.1021/i200021a023.

Michelsen, M.L. 1987. Multiphase Isenthalpic and Isentropic Flash Algorithms. *Fluid Phase Equilibria* **33** (1–2): 13–27. http://dx.doi.org/10.1016/0378-3812(87)87002-4.

Michelsen, M.L. 1993. Phase Equilibrium Calculations. What Is Easy and What Is Difficult? *Computers & Chemical Engin*. **17** (5–6): 431–439. http://dx.doi.org/10.1016/0098-1354(93)80034-K.

Néron, A., Lantagne, G., and Marcos, B. 2012. Computation of Complex and Constrained Equilibria by Minimization of the Gibbs Free Energy. *Chemical Eng. Sci*. **82:** 260–271. http://dx.doi.org/10.1016/j.ces.2012.07.041.

Nghiem, L.X. 1983. A New Approach to Quasi-Newton Methods With Application to Compositional Modeling. Paper presented at the SPE Reservoir Simulation Symposium, San Francisco, California, 15–18 November. SPE-12242-MS. http://dx.doi.org/10.2118/12242-MS.

Nghiem, L.X. and Li, Y.K. 1984. Computation of Multiphase Equilibrium Phenomena With an Equation of State. *Fluid Phase Equilibria* **17** (1): 77–95. http://dx.doi.org/10.1016/0378-3812(84)80013-8.

Okuno, R. 2009. *Modeling of Multiphase Behavior for Gas Flooding Simulation*. PhD dissertation, the University of Texas at Austin, Austin, Texas (August 2009).

Okuno, R., Johns, R.T., and Sepehrnoori, K. 2010. A New Algorithm for Rachford-Rice for Multiphase Compositional Simulation. *SPE J.* **15** (2): 313–325. SPE-117752-PA. http://dx.doi.org/10.2118/117752-PA.

Okuno, R. and Xu, Z. 2014. Efficient Displacement of Heavy Oil by Use of Three Hydrocarbon Phases. *SPE J.* **19** (5): 956–973. SPE-165470-PA. http://dx.doi.org/10.2118/165470-PA.

Peng, D.-Y. and Robinson, D.B. 1976a. A New Two-Constant Equation of State. *Industrial and Engineering Chemistry Fundamentals* **15** (1): 59–64. http://dx.doi.org/10.1021/i160057a011.

Peng, D.-Y. and Robinson, D.B. 1976b. Two and Three Phase Equilibrium Calculations for Systems Containing Water. *Can. J. Chem. Eng.* **54** (6): 595–599. http://dx.doi.org/10.1002/cjce.5450540620.

Poling, B.E., Prausnitz, J.M., and O'Connell, J.P. 2000. *The Properties of Gases and Liquids*, fifth edition. New York: McGraw-Hill Professional.

Prats, M. 1982. *Thermal Recovery*. SPE Monograph Series, Vol. 7. New York: Henry L. Doherty Series.

Rachford, H.H. Jr. and Rice, J.D. 1952. Procedure for Use of Electronic Digital Computers in Calculating Flash Vaporization Hydrocarbon Equilibrium. *Petroleum Trans., AIME* **195:** 327–328. SPE-952327-PA. http://dx.doi.org/10.2118/952327-PA.

Rubin, B. and Buchanan, W.L. 1985. A General Purpose Thermal Model. *SPE J.* **25** (2): 202–214. SPE-11713-PA. http://dx.doi.org/10.2118/11713-PA.

Shu, W.R. and Hartman, K.J. 1988. Effect of Solvent on Steam Recovery of Heavy Oil. *SPE Res Eval & Eng* **3** (2): 457–465. SPE-14223-PA. http://dx.doi.org/10.2118/14223-PA.

Tester, J.W. and Modell, M. 1996. *Thermodynamics and Its Applications*, third edition. New Jersey: Prentice Hall.

Tsonopoulos, C. 1999. Thermodynamic Analysis of the Mutual Solubilities of Normal Alkanes and Water. *Fluid Phase Equilibria* **156** (1): 21–33. http://dx.doi.org/10.1016/S0378-3812(99)0021-7.

Tsonopoulos, C. and Wilson, G.M. 1983. High-Temperature Mutual Solubilities of Hydrocarbons and Water. Part I: Benzene, Cyclohexane and *n*-Hexane. *AIChE J.* **29** (6): 990–999. http://dx.doi.org/10.1002/aic.690290618.

Varavei, A. and Sepehrnoori, K. 2009. An EOS-Based Compositional Thermal Reservoir Simulator. Paper presented at the SPE Reservoir Simulation Symposium, The Woodlands, Texas, USA, 2–4, February. SPE-119154-MS. http://dx.doi.org/10.2118/119154-MS.

Venkatramani, A. and Okuno, R. 2014. Modeling of Multiphase Behavior for Water/n-Alkane Mixtures by Use of the Peng-Robinson EOS. Paper presented at the SPE Heavy Oil Conference-Canada, Calgary, Alberta, Canada, 10–12 June. SPE-170100-MS. http://dx.doi.org/10.2118/170100-MS.

Wagner, W. 1973. New Vapour Pressure Measurements for Argon and Nitrogen and a New Method for Establishing Rational Vapour Pressure Equations. *Cryogenics* **13** (8): 470–482. http://dx.doi.org/10.1016/0011-2275(73)90003-9.

Willman, B.T., Valleroy, V.V., Runberg, G.W. et al. 1961. 1537-G-Laboratory Studies of Oil Recovery by Steam Injection. *J Pet Technol* **13** (7): 681–690. SPE-1537-G-PA. http://x.doi.org/10.2118/1537-G-PA.

Zhu, D. and Okuno, R. 2014. A Robust Algorithm for Isenthalpic Flash of Narrow-Boiling Fluids. *Fluid Phase Equilibria* **379:** 26–51. http://dx.doi.org/10.1016/j.fluid.2014.07.003.

Appendix A—Isenthalpic Flash Formulation

The most fundamental formulation for PH flash is to maximize the total entropy of a closed system at a specified pressure and enthalpy (Brantferger 1991; Brantferger et al. 1991). That is, for a given P, $\underline{H}_{\text{spec}}$, and z_i ($i = 1, 2, \ldots, N_C$), it is to find T and x_{ij} ($i = 1, 2, \ldots, N_C$, and $j = 1, 2, \ldots, N_P$) that maximize

$$\underline{S}^t = \sum_{j=1}^{N_P} \beta_j \underline{S}_j, \quad \ldots\ldots\ldots\ldots\ldots\ldots\ldots\ldots \text{(A-1)}$$

where P is pressure, $\underline{H}_{\text{spec}}$ is the specified molar enthalpy, z_i is the overall mole fraction of component i, T is temperature, x_{ij} is the mole fraction of component i in phase j, $\underline{S}^t$ is the total molar entropy, β_j is the mole fraction of phase j, $\underline{S}_j$ is the molar entropy of phase j, N_C is the number of components, and N_P is the number of equilibrium phases. The following constraints are to be satisfied:

$$z_i = \sum_{j=1}^{N_P} \beta_j x_{ij} \text{ for } i = 1, 2, \ldots, N_C \quad \ldots\ldots\ldots\ldots\ldots\ldots \text{(A-2)}$$

$$\sum_{j=1}^{N_P} \beta_j = 1.0 \quad \ldots\ldots\ldots\ldots\ldots\ldots\ldots\ldots\ldots\ldots \text{(A-3)}$$

$$\underline{H}^t = \sum_{j=1}^{N_P} \beta_j \underline{H}_j = \underline{H}_{\text{spec}}, \quad \ldots\ldots\ldots\ldots\ldots\ldots\ldots \text{(A-4)}$$

where $\underline{H}^t$ is the total molar enthalpy and $\underline{H}_j$ is the molar enthalpy of phase j.

Appendix B—Jacobian Matrix

The elements of the Jacobian matrix for an N_C-component N_P-phase system are

$$\frac{\partial g_j}{\partial T_D} = T_{\text{ref}} \sum_{i=1}^{N_C} \frac{z_i}{t_i^2} \left[t_i K_{ij} \frac{\partial \ln K_{ij}}{\partial T} - (K_{ij} - 1) \sum_{k=1}^{N_P - 1} \beta_k K_{ik} \frac{\partial \ln K_{ik}}{\partial T} \right], \quad \text{for } j = 1, 2, \ldots, (N_P - 1) \quad \ldots\ldots\ldots\ldots \text{(B-1)}$$

$$\frac{\partial g_j}{\partial \beta_k} = -\sum_{i=1}^{N_C} \frac{z_i}{t_i^2} (K_{ij} - 1)(K_{ik} - 1), \quad \text{for } j, k = 1, 2, \ldots, (N_P - 1) \quad \ldots\ldots\ldots\ldots \text{(B-2)}$$

$$\frac{\partial g_{N_P}}{\partial T_D} = T_{\text{ref}} \sum_{j=1}^{N_P} \beta_j \left(\sum_{i=1}^{N_C} \frac{\partial x_{ij}}{\partial T} \frac{\underline{H}_i^{IG}}{\underline{H}_{\text{spec}}} + \sum_{i=1}^{N_C} \frac{x_{ij}}{\underline{H}_{\text{spec}}} \frac{\partial \underline{H}_i^{IG}}{\partial T} + \frac{\partial \underline{H}_{Dj}^{\text{dep}}}{\partial T} \right) \quad \ldots\ldots\ldots\ldots\ldots\ldots \text{(B-3)}$$

$$\frac{\partial g_{N_P}}{\partial \beta_k} = (\underline{H}_{Dk}^{IGM} + \underline{H}_{Dk}^{\text{dep}}) - (\underline{H}_{DN_P}^{IGM} + \underline{H}_{DN_P}^{\text{dep}}), \quad \text{for } k = 1, 2, \ldots, (N_P - 1) \quad \ldots\ldots\ldots\ldots \text{(B-4)}$$

where $t_i = 1 + \sum_{j=1}^{N_P - 1} (K_{ij} - 1)\beta_j$, for $i = 1, 2, \ldots, N_C$. The computation of $\underline{H}_j^{\text{dep}}$, $\underline{H}_i^{IG}$, and $\underline{H}_j^{IGM}$ can be found in Tester and Modell (1996), Poling et al. (2000), and Zhu and Okuno (2014). Pertinent derivatives are

$$\frac{\partial x_{ij}}{\partial T} = \frac{z_i}{t_i} K_{ij} \frac{\partial \ln K_{ij}}{\partial T} - \frac{z_i}{t_i^2} K_{ij} \sum_{k=1}^{N_P - 1} \beta_k K_{ik} \frac{\partial \ln K_{ik}}{\partial T}, \quad \text{for } j = 1, 2, \ldots, (N_P - 1) \quad \ldots\ldots\ldots\ldots \text{(B-5)}$$

$$\frac{\partial \underline{H}_i^{IG}}{\partial T} = C_{P1i}^0 + C_{P2i}^0 T + C_{P3i}^0 T^2 + C_{P4i}^0 T^3, \quad \text{for } i = 1, 2, \ldots, N_C \quad \ldots\ldots\ldots\ldots\ldots\ldots \text{(B-6)}$$

$$\frac{\partial \underline{H}_{Dj}^{\text{dep}}}{\partial T} = \frac{1}{\underline{H}_{\text{spec}}} \left\{ \text{Term 1} \times \ln \left[\frac{Z_j + (1 + \sqrt{2}) B_{mj}}{Z_j + (1 - \sqrt{2}) B_{mj}} \right] + \frac{RT^2 \partial A_{mj}/\partial T + RTA_{mj}}{2\sqrt{2} B_{mj}} \times \text{Term 2} + R(Z_j - 1) + RT \frac{\partial Z_j}{\partial T} \right\}, \quad \ldots\ldots\ldots\ldots\ldots\ldots \text{(B-7)}$$

where C_{P1i}^0, C_{P2i}^0, C_{P3i}^0, and C_{P4i}^0 are ideal-gas heat capacity coefficients for component i. For estimation of C_{P1i}^0, C_{P2i}^0, C_{P3i}^0, and C_{P4i}^0 for pseudocomponents, normal boiling temperatures calculated from the PR EOS are used with the correlation of Kesler and Lee (1976). In Eq. B-7,

$$\text{Term 1} = \left[B_{mj}\left(3RT\frac{\partial A_{mj}}{\partial T} + RT^2\frac{\partial^2 A_{mj}}{\partial T^2} + RA_{mj}\right) - \frac{\partial B_{mj}}{\partial T}\left(RT^2\frac{\partial A_{mj}}{\partial T} + RTA_{mj}\right)\right] \Big/ \left(2\sqrt{2}B_{mj}^2\right) \quad \cdots \text{(B-8)}$$

$$\text{Term 2} = \frac{-[\partial Z_j/\partial T + (1+\sqrt{2})\partial B_{mj}/\partial T][Z_j + (1-\sqrt{2})B_{mj}]}{[Z_j + (1+\sqrt{2})B_{mj}][Z_j + (1-\sqrt{2})B_{mj}]}. \quad \cdots \text{(B-9)}$$

$\partial A_{mj}/\partial T$, $\partial B_{mj}/\partial T$, $\partial^2 A_{mj}/\partial T^2$, and $\partial Z_j/\partial T$ can be found in Zhu and Okuno (2014).

Di Zhu is a PhD degree candidate in petroleum engineering in the Department of Civil and Environmental Engineering at the University of Alberta. Her research interests include multiphase behavior and numerical reservoir simulation. Zhu holds a BS degree from the Yangtze University and an MS degree from the China University of Petroleum (East China), both in geodetection and information technology. She is an SPE member.

Ryosuke Okuno has served as an assistant professor of petroleum engineering in the Department of Civil and Environmental Engineering at the University of Alberta since 2010. His research and teaching interests include enhanced oil recovery, thermal oil recovery, oil-displacement theory, numerical reservoir simulation, thermodynamics, multiphase behavior, and applied mathematics. Okuno has 7 years of industrial experience as a reservoir engineer with Japan Petroleum Exploration Company. and is a registered professional engineer in Alberta, Canada. He holds BS and MS degrees in geosystem engineering from the University of Tokyo and a PhD degree in petroleum engineering from the University of Texas at Austin. Okuno is a recipient of the 2012 SPE Petroleum Engineering Junior Faculty Research Initiation Award. He is currently an associate editor for *Journal of Natural Gas Science & Engineering*.